International Journal of Pharmaceutics 689 (2026) 126473

Contents lists available at ScienceDirect

International Journal of Pharmaceutics

journal homepage: www.elsevier.com/locate/ijpharm

Understanding how exposure to drone-induced vibration during transportation affects the quality of a monoclonal antibody (Nivolumab)

W. Zhu [a], K. Theobald [b], M. Tobyn [c], P. Courtney [a], P.G. Royall [a,*], T. Cherrett [d], T. Waters [b]

[a] Institute of Pharmaceutical Science, Faculty of Life Sciences & Medicine, King's College London, SE1 9NH, UK
[b] Institute of Sound and Vibration Research, Faculty of Engineering and Physical Sciences, University of Southampton, S017 1BJ, UK
[c] Drug Product Development, Global Product Development and Supply, Bristol Myers Squibb, CH4 9QW, UK
[d] Transportation Research Group, Faculty of Engineering and Physical Sciences, University of Southampton, S017 1BJ, UK

ARTICLE INFO

Keywords:
Nivolumab
Monoclonal antibody
Aseptic preparations
Intravenous infusions
Quality assurance
Vibration
Uncrewed aerial vehicle

ABSTRACT

Therapeutic monoclonal antibodies essential for cancer treatments, are sensitive biomolecules requiring reconstitution in infusion bags, and administration within hours. While drone transportation presents a promising solution for reaching remote healthcare facilities, it introduces mechanical stresses that can compromise mAb stability, leading to protein unfolding and aggregation. This study aimed to evaluate the stability of reconstituted Opdivo® (nivolumab) across vibrations modelling flight. Two different reciprocating shakers were used to simulate predominant frequencies of drone-induced vibrations in a controlled laboratory setting, employing analytical techniques (UV, DLS & SE-HPLC) to assess critical parameters and support the development of risk assessments for drone transportation. Nivolumab infusions remained stable under simulated drone vibrations, with all quality attributes meeting acceptance criteria. Samples exposed to varying frequencies 8, 63, 125 Hz for 30 min; 63 Hz for 1, 2, 3 h; a 43-minute drone flight, and prepared at different concentrations (0.48, 0.86, 1.24 mg/mL) showed no significant differences from controls. Two of the three samples subjected to 125 Hz vibration for 30 min exhibited a minor increase in monomer content ($\leq$0.16 %, $p = 0.003$) on Day 2, accompanied by a 3 nm reduction in particle size. However, these changes remained within pharmaceutically acceptable limits and showed no evidence of functional compromise compared to controls. The particle size shift dissipated after 24 h of storage, suggesting a reversible, vibration-induced dissociation of oligomeric species. Understanding, the impact of flight on product characteristics and stability is important. The results show that Opdivo® is not affected by the vibrations generated by the various stages of drone flight. This paper establishes a reproducible framework for evaluating monoclonal antibody stability under simulated transport conditions, contributing to the development of safer and more efficient delivery methods in cancer care.

1. Introduction

Monoclonal antibodies (mAbs), as therapeutic proteins are increasingly used in clinical practice as they have affinity towards specific antigens (Le Basle et al., 2020). Before administration to cancer patients, these medicines are often reconstituted (about 60 %) and stored in infusion bags to achieve the desired dose and form (Luo et al., 2017). These valuable treatments typically have a short shelf-life (hours) and require timely and rapid logistics services to meet patients' needs (Wozniewski et al., 2024).

Drones or uncrewed aerial vehicles (UAVs) have seen increasing use in medical logistics over recent years, but there is little experimental data to support the assumption that medicine stability is not compromised during transportation (Surman & Lockey, 2024; Oakey et al., 2022; Johnson et al., 2021). This transit and subsequent journey to the patient site poses several stability challenges, as transportation is a significant source of mechanical stresses that may induce interface-mediated protein aggregation (Le Basle et al., 2020; Oakey et al., 2021; Ripple and Dimitrova, 2012).

The interfacial mechanical stress within infusion bags is affected by the presence of air, commonly referred to as headspace (Linkuvienė et al., 2022; Wu et al., 2020; Sreedhara et al., 2012). Even if the medicine solution were added on the overfilled volume (i.e. 105–115 mL fill range of 100 mL labelled IV bag) (Baxter, 2024), the headspace would

* Corresponding author at: Institute of Pharmaceutical Science, Faculty of Life Sciences & Medicine, King's College London, SE1 9NH, UK.

https://doi.org/10.1016/j.ijpharm.2025.126473
Received 12 March 2025; Received in revised form 3 December 2025; Accepted 4 December 2025
Available online 7 December 2025

not be removed (i.e. by removing air) after the preparation to mitigate the air–liquid interface (Theobald et al., 2023). Furthermore, dilution of protein products in IV solution typically results in a decrease in the concentrations of excipients (e.g., surfactants) to levels below those that are needed to stabilise proteins from aggregation. With inadequate surfactant levels in the IV solution, proteins can adsorb more easily to air–liquid interfaces and form films because of their partial amphiphilic nature (Wozniewski et al., 2024). These films can be ruptured by mechanical stress and contribute to aggregate, and particulate released into to the bulk solution (Cohrs et al., 2024; Koepf et al., 2018; Rabe et al., 2011). Moreover, excessive mechanical stress during the handling of the diluted product can directly cause the formation of antibody aggregates (Randolph et al., 2020; Gerhardt et al., 2014; Linkuvienė et al., 2022).

There are only limited vibration exposure tests available for vibrational stability screening. The influence of vibration during transportation, validated by benchtop experiments, is not currently part of typical medicine stability testing frameworks and there are very few guides or operating procedures (Oakey et al., 2021). Forced degradation studies using orbital shakers and vortex mixer are widely used to evaluate stability against vibration stress (Ghazvini et al., 2016). The frequency and amplitude of the acceleration are related to the rotation speed, which is limited, typically to 3000 rpm and 2g respectively. Furthermore, the vortex induced motion of the liquid is not representative of translational agitations observed during transportation for which the motion is random in each direction (Oakey et al., 2021).

Vibration during drone transportation differs from traditional modes of transportation (e.g., rail, road) particularly in relation to frequency, which can occur at significant magnitudes above 200 Hz during take-off and landing, see Table 1 & Zhu et al., 2023. To date this vibrational range has not been extensively studied (Ghazvini et al., 2016). In addition, actual flight trials are typically costly and difficult to carry out due to the challenges of gaining aviation regulatory approval (Stierlin et al., 2024), so it is necessary to conduct accessible simulation experiments in labs.

A widely accepted approach is the use of transport simulators for random vibration testing. These tests incorporate critical parameters such as container volume, orientation, temperature and protein concentration, and are considered the most reliable method for predicting the effects of real-time shipping conditions (Oakey et al., 2021). Fleischman et al. (2017) developed such a test with an acceleration magnitude correlating to the transportation process of less than 6 g, which is in line with the American Society for Testing and Materials standard D4169. This test successfully simulated micron aggregate (diameter, 1–100 μm, also called subvisible particles) behaviour during actual shipment for several monoclonal antibodies in vials and prefilled syringe configurations (Kizuki et al., 2022). However, the range of

Table 1
Previous involved drone experiment data.

Drone model	Drone picture	Drone Taxonomy	Predominant Octave Band (Centre Frequency)	Test duration	Payload	Reference
Windracers – Ultra		Petrol Fixed wing	32 Hz	82 mins 111 mins	Insulin for injection (*Actrapid*®, 10 mL/vial) Water in 360 mL IV bags	(Oakey et al., 2021)
Skylift – V50 (Mugin 5 Pro)		VTOL Fixed Wing	125 Hz	2 mins 6 mins 10 mins	Bevacizumab (*Avastin*®, in 100 mL IV bags) Trastuzumab (*Herceptin*®, in 250 mL IV bags) Rituximab (*Truxima*®, in 500 mL IV bags)	(Zhu et al., 2023)
Skyports – Kookaburra		VTOL Fixed Wing	250 Hz	≈ 61 mins	Normal Saline in 500 mL IV bags	(Wiltshire et al., 2024)
Motion Robotics – Arty		Multi-copter	63 Hz	17 mins	Insulin for injection (*Actrapid*®, 10 mL/vial) Water in 360 mL IV bags	(Oakey et al., 2021)
Plymouth Rock -X1		Multi-copter	250 Hz	2 – 4 mins (60 flights)	Rituximab (*Truxima*®, in 500 mL IV bags) Trastuzumab (*Herceptin*®, in 250 mL IV bags)	(Theobald et al., 2023)
Soton UAV – Spotter		Petrol Fixed Wing	125 Hz	43 mins	Nivolumab (*Opdivo*®, in 100 mL IV bags)	This paper

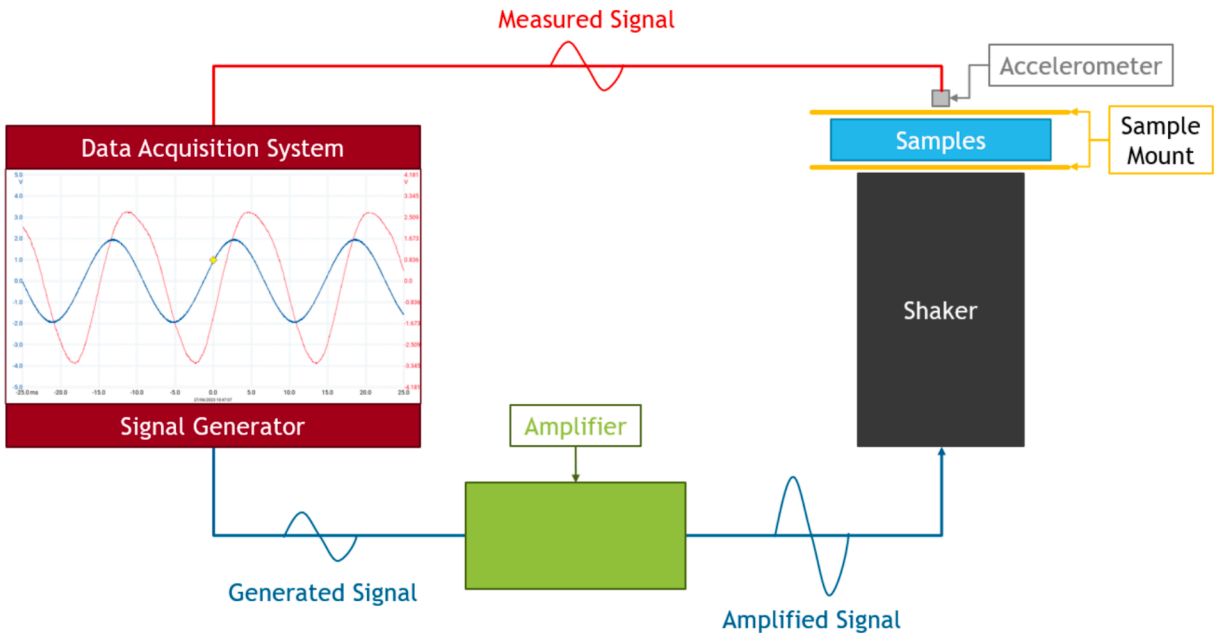

Fig. 1. Illustrative diagram of the standard shaker equipment set-up.

Table 2
Summary of key parameters of the two proposed shakers.

	APS 400	The Modal Shop 2110E
Vibration Mode	Long Stroke Linear Bearing	Electrodynamic
Minimum Frequency (to achieve 2 g)	3 Hz	6 Hz
Maximum Frequency	200 Hz	6,000 Hz
Minimum Amplitude (Bare Table)	1.2 g	1.3 g
Maximum Amplitude (Bare Table)	14.7 g	110 g

magnitudes and frequencies required for developing analogous drone transportation tests needs to be adjusted to cover typical drone flight conditions.

Few studies have investigated the impact of drone transport on mAb stability, with only one recent publication by Güngören et al. (2024) addressing this for a different set of antibodies outside of those investigated in the recent work by the authors. In this paper, the authors are the first to model and replicate drone-induced vibrations from multiple platforms in the laboratory. By enabling future simulation of drone transport conditions without actual flights, the work offers a practical tool for pharmaceutical scientists. It supports the design of more robust formulations and contributes valuable new knowledge to a growing field.

The international clinical relevance of using Nivolumab as a model drug for this drone transport study is demonstrated by its inclusion in the World Health Organization's Essential Medicines List. Although typically administered in hospital settings, patients in remote or underserved regions, such as the Scottish and Greek islands, and other geographically isolated areas, face challenges in accessing timely treatment. This study aligns with current healthcare transformation initiatives, including the Transforming NHS Pharmacy Aseptic Services in England report, which advocates for centralized reconstitution of high-value aseptic products and decentralized administration. The work addresses the logistical need to deliver prepared infusions within a limited stability window, as recommended by the European Medicines Agency. While emergency medications fall outside the scope of this study, the simulated drone transport framework developed here offers a practical method for evaluating vibration-related risks, with potential future application to a wider range of time-sensitive therapies.

The aim of this study was to test the physio-chemical stability of Opdivo® (Nivolumab) reconstituted in intravenous (IV) bags exposed to bench simulated drone vibration and quantify any potential effects on their stability. The findings contribute to the development of a reproducible framework for future testing of the suitability of drone platforms and the vibrational failure limits of medical products.

2. Methodology

2.1. Experimental development

In accordance with standard industry vibration testing procedures, vibration should be imparted to the samples through the use of a shaker (e.g., ASTM D4169). Commercially available shakers are almost exclusively uniaxial, i.e. simulate motion in a single direction. These are applicable to the replication of drone vibration when the vertical direction is observed to predominate, see (Oakey et al., 2021) for example.

A standard vibration testing laboratory set up (Fig. 1) was adopted comprising a data acquisition system (DataPhysics Abacus 901) hosted by a laptop which both generates the desired excitation signal and acquires the acceleration of the shaker using an accelerometer (e.g., PCB Piezotronics 2050E09) to ensure that the signal has been faithfully replicated. The excitation signal passes through a dedicated power amplifier to drive the shaker. The samples were held in place using a bespoke sample mount.

2.1.1. Single frequency studies (studies 1–3)

The first three studies used single level sinusoidal excitation at discrete frequencies to provide a precise and controlled method for investigating the effects of vibrations on monoclonal antibodies. Further

details of the study structure are provided in Table 2.

2.1.1.1. Selection of frequencies. The selection of the test frequencies has been determined based on the findings of several live flight trials that have been undertaken using a range of drone platforms (see Table 1).

The methodology for recording vibration profiles of drone transported cargo has been previously developed through several earlier studies (Theobald et al., 2023; Zhu et al., 2023; Oakey et al., 2021). These trials have undertaken a range of analyses on the vibration profiles of several different drones. Table 1 provides a high-level comparison of these trials and the key parameters of each of the flights.

Based on a review of these findings, dominant drone frequencies vary between platforms, but predominantly fall within the 32 to 250 Hz octave bands (Table 1). This range captures the most relevant vibrational stressors observed across fixed-wing and multi-copter drone flight trials (Fig. 2). While some traditional transport modes (e.g., vans and cars) typically generate lower-frequency vibrations, often below 10 Hz (Oakey et al., 2021), the selected frequency range reflects the higher-frequency spectrum more characteristic of drone operations. It also aligns with the operating range of the APS400 vibration shaker used in this study (as detailed in Section 3.3), ensuring practical feasibility and reproducibility.

The frequencies 8 Hz, 63 Hz, and 125 Hz were selected as discrete test frequencies. 8 Hz represents a low-frequency boundary to capture baseline sensitivity and serve as a comparison to conventional transport. 63 Hz and 125 Hz correspond to central frequencies within the most commonly reported dominant octave bands in drone vibration studies. Although 250 Hz has also been identified in recent literature (Wiltshire et al., 2024; Theobald et al., 2023), it was excluded from initial tests due to limitations in the shaker system's performance at that frequency.

2.1.1.2. Selection of duration. The durations of vibration for the experiments reported in this paper were selected to best replicate the durations of real flights, ranging from 30 mins to 180 mins which represent distances of approximately 12 km to 70 km estimated by average drone speed, which is based on the average speed of the drone flight discussed in study 4, in section 3.2.

2.1.2. Flight replication study (Study 4)

The signals used in Study 4 were taken from vibration measurements of a real flight. The drone platform used in this example test was the Soton UAV 'Spotter' which is a fixed-wing drone platform (Fig. 3(a)) powered by two single cylinder, four-stroke petrol engines.

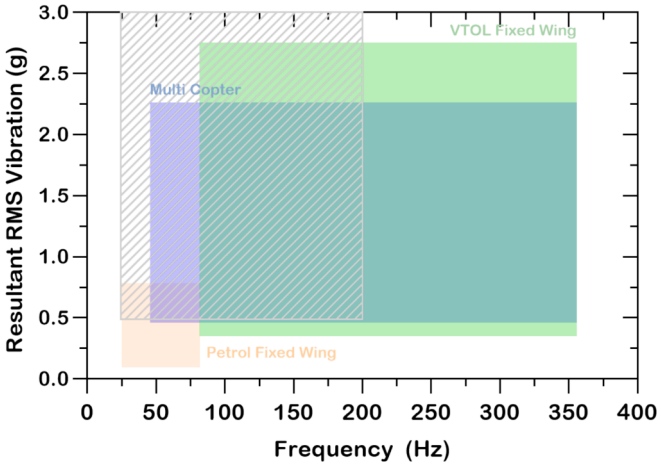

Fig. 2. Illustrative graph of typical Root Mean Squared (RMS) vibration levels measured during live drone flight trials. The target environment for the laboratory trials is indicated by a grey hatch.

The flight was undertaken at Draycot Farm Aerodrome GB-0006, lasting 43 min, it followed both clockwise and anticlockwise circuits at a constant altitude of 110 m covering a distance of approximately 17 km (Fig. 3(b)).

The payload containing the samples was an instrumented tube carrier (Fig. 4(b)), which was underslung from the fuselage (Fig. 3(a)). The tube was a standard medical carrier known as a BIO-BOTTLE® (COMP07, Bio-packaging) which is a rigid high-density polyethylene bottle typically used to carry patient samples. The loaded bio-bottle is shown in Figure (c) and has similar dimensions to the containers used in hospital pneumatic tube systems.

Vibration recording was undertaken using the same methodology as previous trials (Theobald et al., 2023). The sensors, triaxial MEMS data logging accelerometers, were mounted directly on the airframe and within the payload to provide a reference for the input vibration to the sample. The sensor positions are shown in the images in Figure.

The signal selected for replication in the laboratory (Study 4) was the recording from within the bio-bottle. This represented the worst-case input due to the overall vibration levels being higher than those recorded on the airframe. This was the most conservative assumption in the case of the sensitive cargos. The vertical direction of the recording was replayed for the full duration of 43 min to facilitate comparison to the real flight.

2.1.3. Selection of the shakers

Reciprocating shakers widely used for pharmaceutical applications are inherently capable of exciting only one frequency at a time (Dasnoy et al. 2024). Whilst adequate for Studies 1 to 3, study 4 requires replication of actual vibration profiles from flight tests for which a shaker is needed that can replicate arbitrary motions comprising many frequencies simultaneously. To meet this need, a mechanical engineering shaker capable of broadband excitation was selected. A target frequency performance range of 2 to 200 Hz and a target vibration magnitude of approximately 2 g were chosen, based on live flight trial vibration data in study 4 (not shown).

At low frequencies, the amplitude of excitation of such shakers is limited by their maximum displacement. An APS 400 long stroke shaker (Fig. 5(a)) was utilised for the initial phase of testing as this shaker can deliver frequencies as low as 2 Hz and up to a maximum value of 14.7 g at higher frequencies, dependent on the mass of the payload. The performance graph for this shaker with several payload configurations can be seen in Fig. 5(c) which shows the maximum achievable acceleration level as a function of frequency.

Throughout testing it was necessary to increase both the magnitude of vibration and/or the frequency range to attempt to induce failure in the medicine payloads. To achieve this, the Modal Shop 2110e shaker (Fig. 5(b)) was used which offers a broader range of performance at higher frequencies, as evident from the payload curves in Fig. 5(c). The modal shop 2110E shaker allowed testing to be conducted at frequencies above 5 Hz and at magnitudes up to a peak acceleration of 55 g.

A comparison of the key parameters of the two shakers can be seen in Table 1 given below.

2.1.4. Experiment procedure

The commercial mAb medicine Nivolumab (Opdivo®, 10 mg/mL concentrate for solution for infusion) was provided by the original manufacturer Bristol Myers Squibb. All infusions were handled according to the manufacturer guidelines (BMS, 2024) as stated in the Summary of Product Characteristics (SmPCs). The vibration testing was conducted at the University of Southampton (Soton) and pharmaceutical testing at King's College London (KCL). The mAbs were transported between Soton and KCL under temperature-controlled conditions (2–8 °C). The average travel time between the two sites is 1.5 h for the single journey.

Two control samples were put in place to account for the impact of natural degradation after preparation (dilution) which was called "KCL

(a) (b)

Fig. 3. (a) Soton UAV Spotter drone used for this trial. (b) Flight path for flight testing at Draycot Airfield. The flight was 43 mins in duration covering approximately 17 km. Base map and data from OpenStreetMap and OpenStreetMap Foundation.

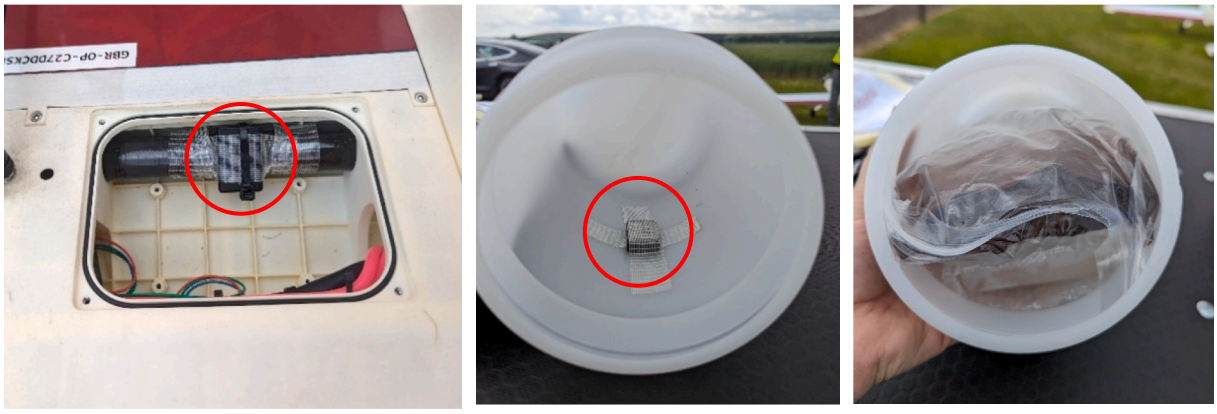

(a) (b) (c)

Fig. 4. (a) Airframe sensor position. (b) Payload sensor poistion. (c) Loaded biobottle with Nivolumab preparations in IV bags.

control" and transport between the two sites for all test infusions which was called "Soton control". The underlined variables in the bulleted list below are given as examples (e.g., 0.86 mg/mL is one of the concentrations studied in the range), full details can be found in Table 3 later in section 3.5. RT/RL: room temperature/room light (Storage at 20 °C to 25 °C and exposed to visible light of approximately 1000–1100 lx).

(1) Day 1: Aseptically prepare five nivolumab 0.86 mg/mL infusions in Sodium Chloride 0.9 % w/v (Baxter, Intravenous Infusion BP, 100 mL, FE1307G). For example, 10 mL of 10 mg/mL nivolumab adds to 106 mL saline solution in VDLF Cabinet. One is the KCL control (stored at 4 °C); one other is the Soton control (always stores alongside the test infusion following the identical temperature profile as the vibrated samples on the shaker); the rest are the test infusions will undergo vibration applied by the shaker. Fig. 6 gives a diagram to simplify the control set up, Fig. 7 shows the aseptic preparation process with essential material information.
(2) Day 1: test all infusions by removing 5 mL from the bag for all analytical techniques described later in section 3.6.
(3) Day 2: transfer the four nivolumab infusions to lab in Soton by train and bus.
(4) Day 2: fix the test infusion on the shaker (Figs. 8 & 9) and shake for 30 min at 63 Hz under RT/RL. Temperature monitored by NHS approved data loggers (EL-USB-2-LCD); infusion bags have been protected from light exposure throughout this process.
(5) Day 2: transfer the four nivolumab infusions to KCL by train and bus. Test all infusions with the same analytical techniques as described in section 2.1.6.
(6) Day 2: store the four infusions at 4 °C for an additional 20 h, then RT/RL for 4 h.
(7) Day 3: at the end of the 24 h of storage, test samples with the analytical techniques as described in section 3.6.

2.1.5. Study design

The original concentrated medicine contained 100 mg Nivolumab in 10 mL solution per vial. Normal saline has been used as diluent for all samples, which was packed in a PVC/DEHP bag. The product preparation accounted for the volume overage in the 100 mL 0.9 %w/v Sodium Chloride Intravenous Infusion bags (overage volume 6 mL, measured with n = 3), to produce final strengths of Nivolumab medicines.

Following standard aseptic practice (NHS, 2023), some units were prepared without accounting for the volume overage. In such cases, the actual sample strength would be 100 mg/116 mL rather than 100 mg/110 mL, this is equivalent to 0.86 mg/mL as a result a 0.91 mg/mL

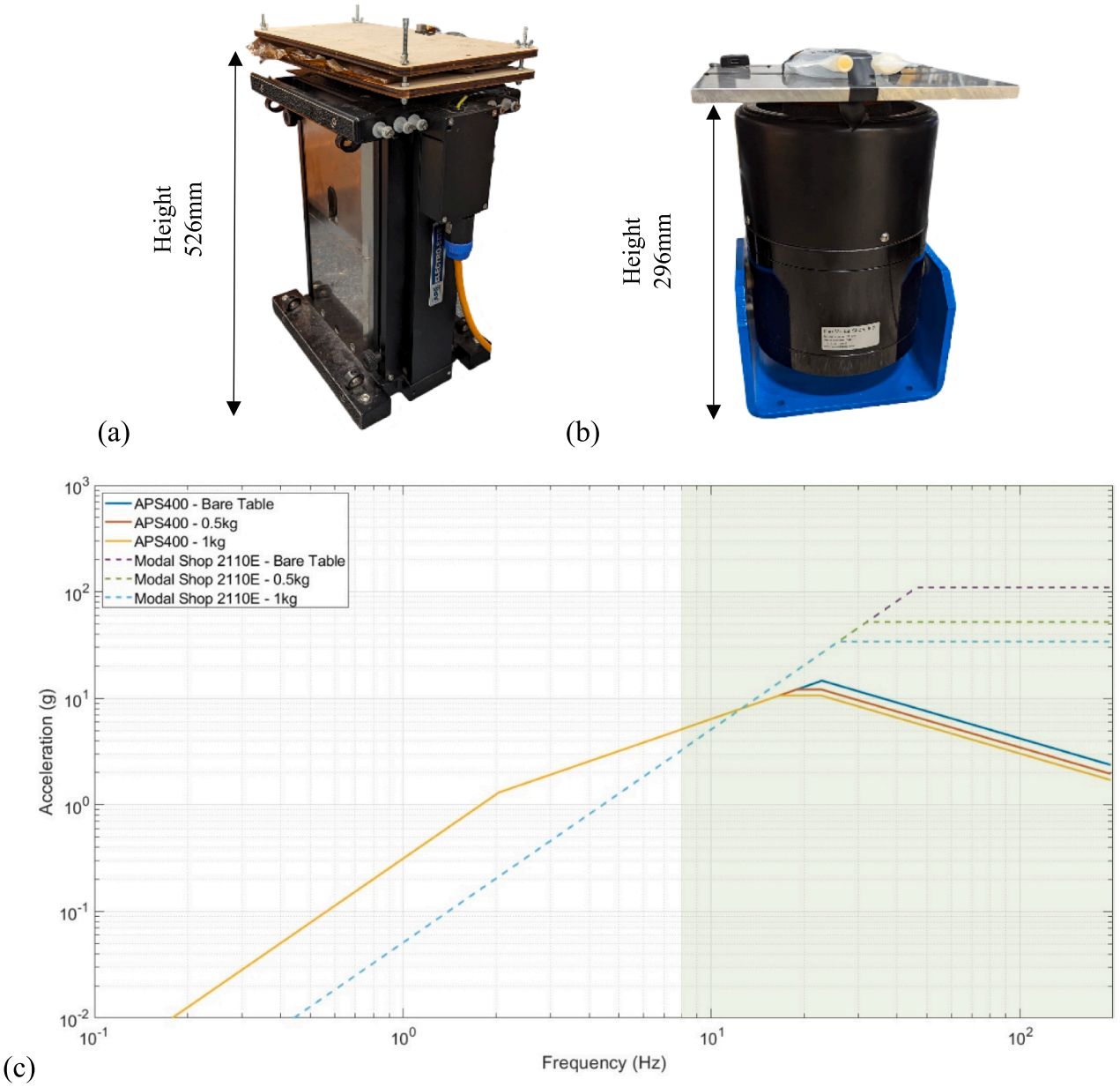

Fig. 5. (a) APS 400 Shaker set up for testing (b) Modal Shop 2110e Shaker set up for testing (c) Annotated payload curve for APS 400 shaker (APS, 2023) and Modal Shop 2110e shaker (THE MODEL SHOP, n.d.) with proposed 8–200 Hz range shaded in green.

Table 3
Plan for shaker simulation study.

Variables	Study 1	Study 2	Study 3	Study 4
Nivolumab concentrations	0.86 mg/mL (100 mg/116 mL)	0.86 mg/mL (100 mg/116 mL)	1.24 mg/mL (150 mg/121 mL) 0.86 mg/mL (100 mg/116 mL) 0.45 mg/mL (50 mg/111 mL)	0.86 mg/mL (100 mg/116 mL)
Frequencies	8 Hz 63 Hz 125 Hz	63 Hz	63 Hz	According to vibration profile
Durations	30 mins	60 mins 120 mins 180 mins	30 mins	43 mins
Scenarios	Shaker	Shaker	Shaker	Shaker & drone

Note: NS stands for Normal Saline, 0.9 % Sodium Chloride Infusion; PES stands for polyether sulfone.

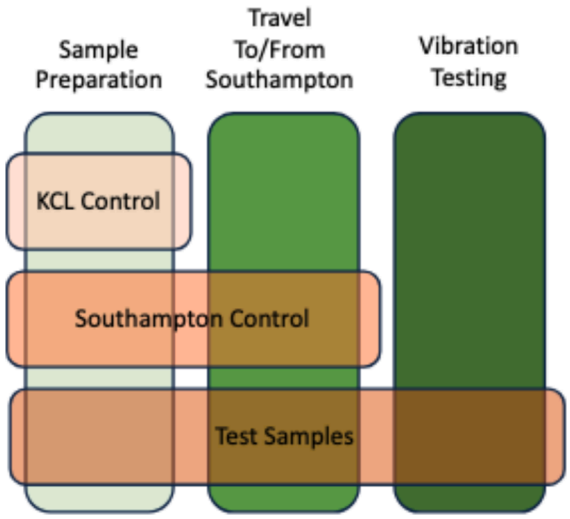

Fig. 6. Schematic diagram of the use of two control samples.

product prepared in this way is covered by this study. Similarly for the 50 mg/111 mL and 150 mg/121 mL samples. Table 3 explains the research plan for different important variables.

2.1.6. Pharmaceutical analyses

All Nivolumab samples underwent visual inspection, protein concentration measurements, pH assessments, Dynamic light scattering (DLS), and Size-Exclusion High-Performance Liquid Chromatography (SE-HPLC) tests. These tests are selected based on aggregation detection recommended in NHS guidance (Santillo et al., 2021). Each method was validated for its ability to detect changes induced by temperature, pH, or vibration during forced degradation analysis.

For the visual inspection, vials were gently wiped and inspected against a non-glare black and white background for 5 s under gentle swirling. Protein concentrations were determined using a Lambda 365 UV/Vis Spectrophotometer (Perkin Elmer) by measuring absorbance at 280 nm, with the absorption coefficient of 1.68 provided by the manufacturer BMS. Sample pH was measured using a Hanna Instruments HI-2020 edge hybrid multiparameter system. DLS measurements were performed in triplicate using a NanoZS90 ZetaSizer (Malvern) with a refractive index of 1.45.

In the SE-HPLC study, all samples were run in triplicates with AdvanceBio SEC 300Å column (Agilent, 4.6 × 150 mm, 2.7 µm, PL1580-3301) at 25 °C. The mobile phase comprised 0.1 mM potassium phosphate buffer and 0.2 mM potassium chloride (pH = 7.0). Elution was detected at 280 nm with a reference wavelength at 360 nm. Before analysis, samples were filtered using Sartorius Minisart® 0.2 µm syringe filters (PES, 15 mm, 1776D).

Detailed operational conditions for the UV spectrophotometer, DLS, and SE-HPLC are provided in Appendix Tables A1, A2, and A3. Readers can refer to the appendix for additional instrumental settings and a comprehensive overview of the pharmaceutical analysis methodology.

All data of UV A_{280} protein concentration, DLS and SE-HPLC were presented as mean ± standard deviation (SD). The statistical significance of differences between groups was determined by one-way analysis of variance (One-way ANOVA) tests and Student's t-tests (two-tailed) on UV and SE-HPLC analysis. The results were considered non-significant when the value of p was ≥ 0.05, significant when $p < 0.05$. "***" indicates $p < 0.001$, "**" indicates $p < 0.01$ and "*" indicates $p < 0.05$.

The acceptance criteria are as follows:

1. Appearance and pH: There should be no physical change in appearance and no significant change in pH (defined as a change of >0.5 pH unit) (Santillo et al., 2021).
2. Protein Concentration by Ultraviolet Spectrophotometry (UV): It has not been clearly defined in the literature; thus, the concentration limits were set based on the 5 % variation on the mean concentration of five Nivolumab samples after preparation (day 1) (Santillo et al., 2021).
3. Dynamic Light Scattering (DLS): A deviation greater than 1 nm from the hydrodynamic diameter of the representative population of the mAbs was out of specification (Guyader et al., 2020). Similarly, the occurrence of another population with an intensity percentage greater than 10 % was also considered out of specification (Malvern, 2013). The population was considered mostly monodisperse when the PDI was ≤0.3 as the reversible aggregates (e.g., dimer) would be formed during manufacturing (Falke & Betzel, 2019; Goldberg et al., 2011).
4. Size Exclusion High Performance Liquid Chromatography (SE-HPLC): the maximum acceptance criteria are a 5 % loss in active protein and a maximum 2 % relative to the main peak increase in any degradant peaks. Specifically, high molecular weight species (HMWS) and low molecular weight species (LMWS), Theobald et al., (2023).

3. Results

3.1. Vibration analysis

A typical recording from the data aquisition system of the actual signals recorded during sinusoidal vibration testing is shown in Fig. 10. While the minimum target amplitude for the selection of the equipment was 2 g, accelerations greater than that have been achieved. The amplitude of the acceleration of the 8 Hz component is 6.6 g, the 63 Hz component is 1.8 g and the 125 Hz is 2.3 g. The total harmonic distortion (THD) is a measure of how much a signal has distorted from the original single frequency signal. For each of these examples the value of THD is, 14.6 %, 7.1 % and 7.0 %.

3.2. Pharmaceutical analysis

The pH of Nivolumab preparations remained at 6.0 ± 0.2 for samples at all conditions, the solutions remained clear, colourless without visible participants. The results of visual inspection and sample spectrum of UV, DLS, SE-HPLC could be found in the Appendix Summary of quality assessments data. After preparation, the Nivolumab had an initial particle

Fig. 7. Aseptic preparation procedure of Nivolumab 0.91 mg/mL in 0.9 % Sodium Chloride. The following medical consumables have been applied. Becton Dickinson Microlance™ 3 needle, 19G (1.1 × 40 mm), 301500; Becton Dickinson Plastipak™ syringe, 10 mL, 305959; Braun Venofix® Safety winged IV needle, 19G (1.1 × 19 mm), 4056505-01.

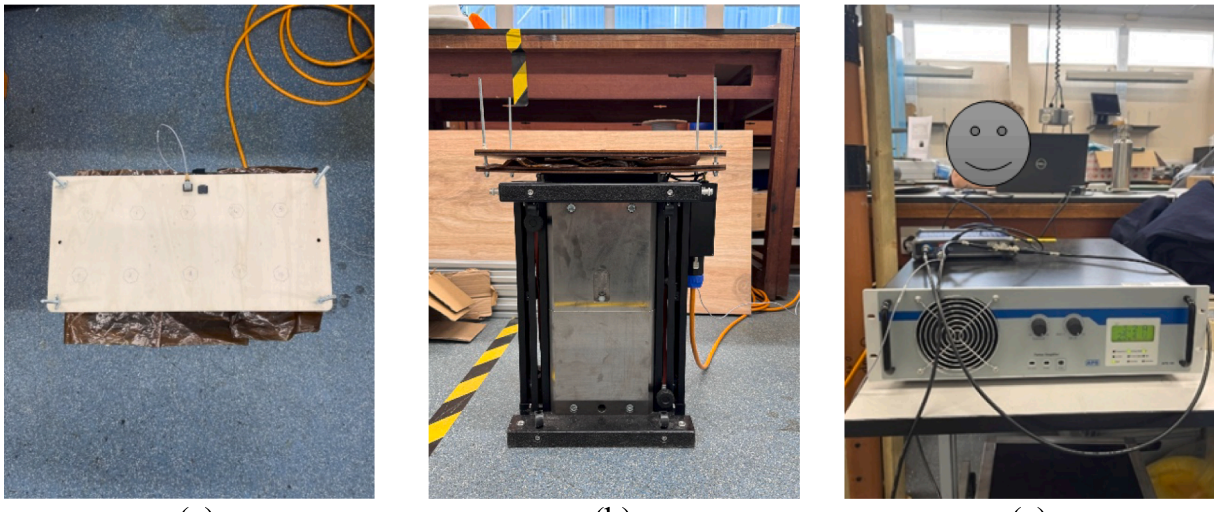

Fig. 8. Drone vibration exposure experiment on APS400 shaker (a) Top view of sample affixed to shaker table with custom sample mount, (b) Side view, (c) APS Dynamics APS145 Spektra V2 amplifier.

Fig. 9. Drone vibration simulation experiment on The Modal Shop shaker (a) Top view of sample affixed to shaker table with adhesive tape (b) Side view, (c) Modal Shop 2050E09 Power Amplifier.

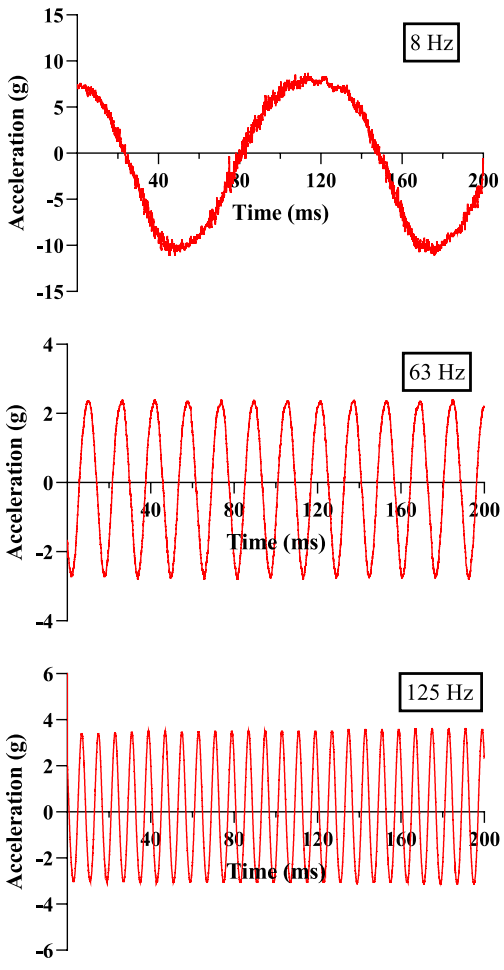

Fig. 10. Measured shaker vibration signal for each frequency in Study 1.

size of 11–14 nm, with a polydispersity index of PDI < 0.2 which was consistent with the literature and the solution contained mostly monomer and a minor population of dimers (Stetefeld et al., 2016). The SE-HPLC demonstrated that the Nivolumab usually has high molecular weight species (HMWS, aggregates) of 0.5 %, monomer of 99.0 % and low molecular weight species (LMWS, fragments) of 0.5 %. The above results matched the findings of Guyader et al., (2020) and Torrente-López et al., (2022) who analyzed the vibration of other mAbs of similar structure.

The protein concentration estimated by UV absorbance at 280 nm was expected based on the predicted or theoretical concentrations of 0.45, 0.86 and 1.24 mg/mL respectively, but the variance in a small number of cases approached 5 %. This was be attributed to experimental errors in the determination of the overage volumes, and manual dilution factors. Overall protein concentration remained within the permitted pharmacopeia limits (Santillo et al., 2021).

In the SE-HPLC analysis, there was a non-assigned chromatographic peak detected at a retention time of 6.72 ± 0.03 min, after the LMWS peak in all chromatographic profiles. However, this peak was not a sign of degradation as it was also detected in the control (fresh) samples, therefore was not included in integration. It was suggested that this peak is only present in diluted product with 0.9 % NaCl by other researchers (Torrente-López et al., 2022).

3.2.1. Study 1 (frequency), 2 (duration), 3(concentration)

In study 1, triplicate samples experienced 8 Hz, 63 Hz or 125 Hz vibration for 30 min. The appearance (Table A1 in Appendix), pH (Table A1 in Appendix), concentration (Fig. 11) and DLS (Fig. 12) results clearly show negligible variations, with all in the acceptance criteria. The SE-HPLC results (Fig. 13) reveal two samples (125 Hz (1), 125 Hz (3)) have shown similar monomer content increase in SE-HPLC analysis after vibration ($p = 0.008$, $p = 0.007$) and extra 24 h storage ($p = 0.03$, $p = 0.03$). Even if the increase (less than 0.16 %) is significant statistically, it still meets the acceptance criteria of 5 % (Santillo et al., 2021). The findings suggest that even at the highest frequency vibration tested (125 Hz), Nivolumab exhibits strong tolerance to mechanical stress over 30 min. However, given the unexplained nature of the monomer shift, further investigations are warranted to differentiate between real structural changes and analytical variability (see Fig. 14) .

In study 2 (results can be found in the Table A2 in appendix), triplicate samples experienced 60 mins, 120 mins or 180 mins vibration at 63 Hz. The appearance, pH, concentration, DLS and SE-HPLC results clearly show negligible variations and within acceptance criteria. The SE-HPLC results show that more HMWS (aggregates) content has been found in a few samples (60 mins (3), 120 mins (3) & 180 mins (2)), but

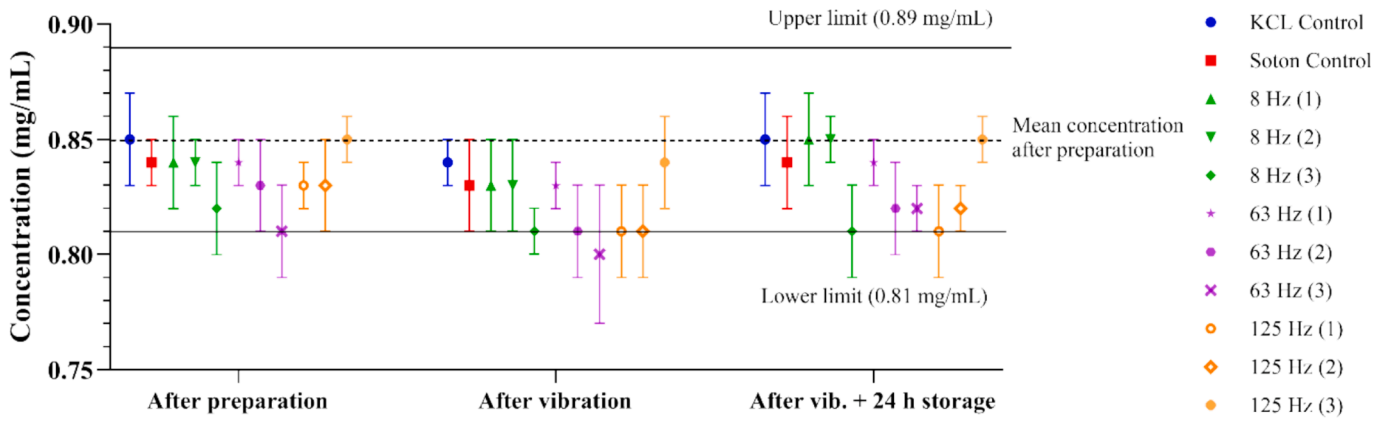

Fig. 11. Concentration of the Nivolumab samples (0.86 mg/mL in 0.9 % w/v NaCl) in the infusions exposed to different vibration frequencies for 30 min within the three-day test. The upper and lower limits are set by ±5 % variation of mean concentration of all 11 samples.

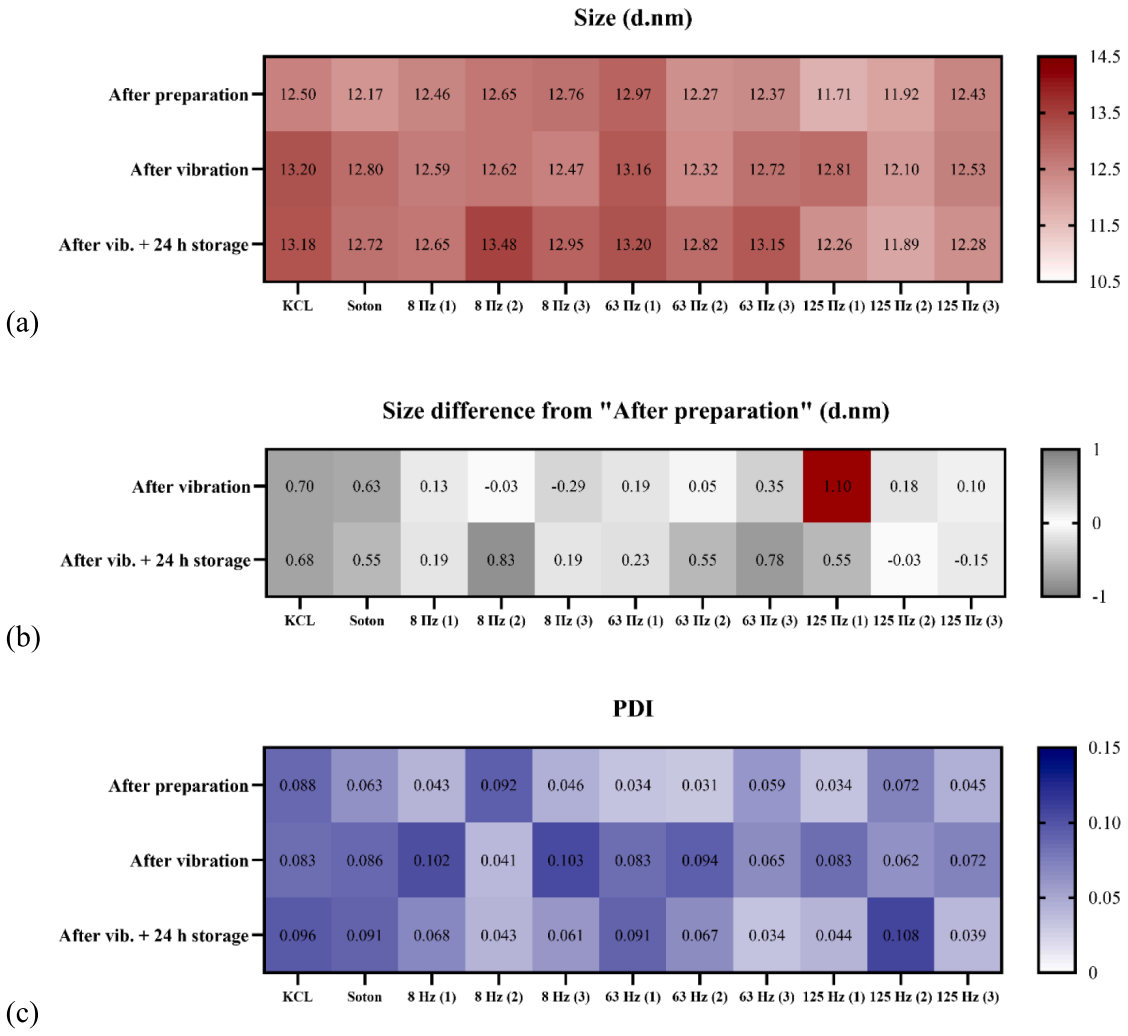

Fig. 12. DLS results of Nivolumab samples (0.86 mg/mL in 0.9 % w/v NaCl) in the infusions exposed to different frequencies vibration for 30 min within three-day test. (a) Z-average size (nm). (b) Z-average size difference from "after preparation" measured on Day 1. (c) PDI. Acceptable range. Hydrodynamic size variation <1 nm, PDI < 0.3. KCL: the "KCL control" sample, Soton: the "Soton" control sample.

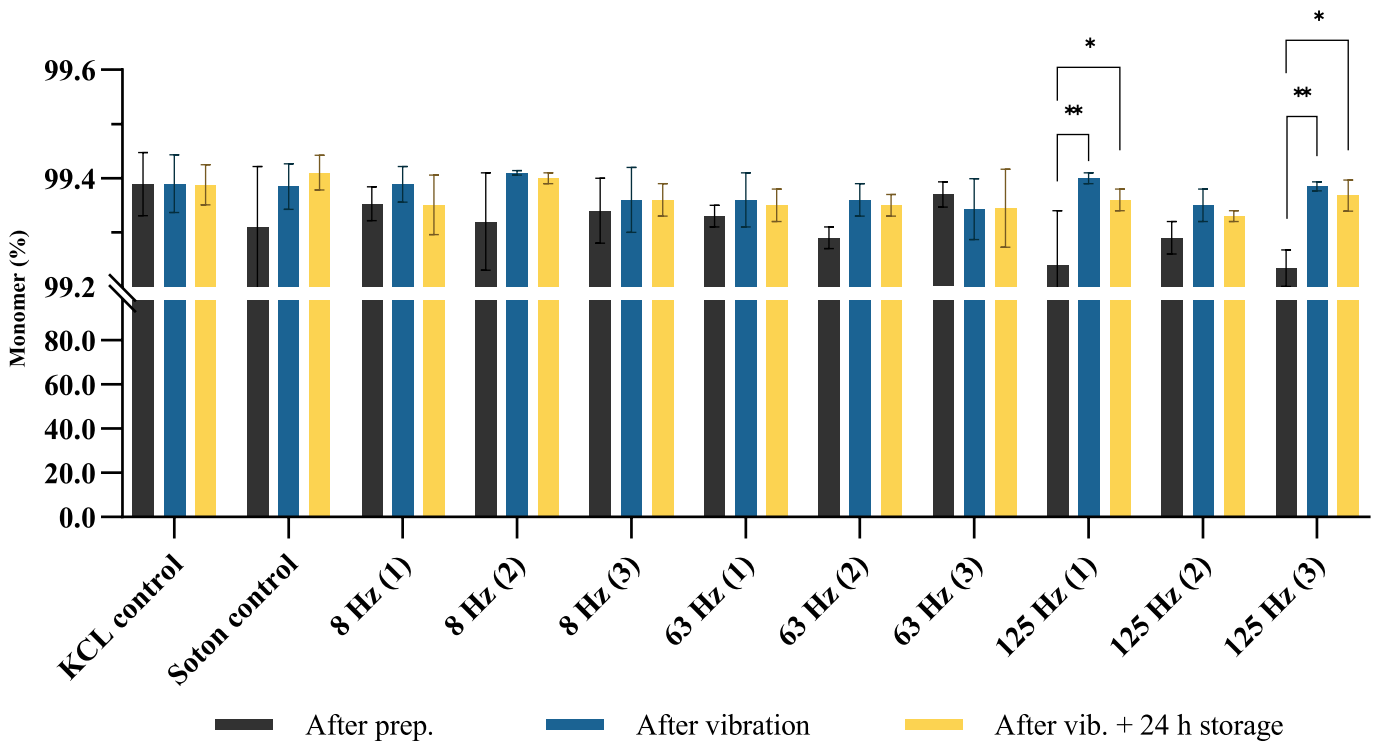

Fig. 13. Monomer content of Nivolumab samples (0.86 mg/mL in 0.9 % w/v NaCl) exposed to different vibration frequencies for 30 min. Data as shown as mean ± SD (n = 3). '*' stands for $p < 0.05$, '**' stands for $p < 0.01$.

the difference is non-significant ($p > 0.05$) and less than 0.1 % which is the typical limit of quantification. Moreover, an increase of aggregates has not been detected on the other two experimental samples in the same conditions. This result shows an assurance of the stability in three hours flight, with 63 Hz being the most predominant frequency (see Fig. 15).

The concentration investigated in study 3, ranging from 0.45 to 1.24 mg/mL, has not found any difference in stability result from typical drone flight vibration (63 Hz 60 mins). The concentration did not contribute to any of the particle size change in DLS and monomer content determined by the elution profile of SE-HPLC.

3.2.2. Study 4 (drone fly trial and simulation on shaker)

Upon subjecting IV bags containing mAbs to drone transport, statistical analysis revealed no significant differences between the control group and vibration-exposed group for Nivolumab.

The SE-HPLC analysis of those infusion bags revealed monomer quantities comparable to the previous three studies. This characteristic remained consistent under both shaker and drone flown groups, indicating a stable and uniform monomeric profile across the different vibration modes (see Fig. 16).

The DLS data showed notable changes in the particle size of Nivolumab after vibration, with the Z-average decrease around 1.5 nm, out of the acceptance criteria of 1 nm size difference (Guyader et al., 2020). However, this change is reversible through the observation of size reform to 13.5 nm after extra 24 h storage at 4 ℃ plus 4 h storage at 25 ℃.

4. Discussion

It is generally acknowledged that two possible processes exist for the generation of protein aggregates during the transportation of IV bags: either the mechanical shock ruptures the protein films at interfaces with insufficient surfactant after dilution, or the bag material induces cavitation at interfaces (Cohrs et al., 2024). For instance, liquid droplets of antioxidants and/or water-immiscible plasticizers emerge from the IV bag material and enter the solution (Linkuvienė et al., 2022).

Our research focused on the frequency, duration and concentration parameters under practical application situations (i.e., overfilled IV bag with limited headspace) with a greater emphasis on real-world case studies. As a result, it is possible that the mechanical stress (vibration) is insufficient to affect the critical quality attributes. Furthermore, it might be more interesting to examine the "swipe area" (the potential movement area of the protein solution under amplitude, acceleration and direction) of various frequencies of an IV bag filled with the same volume of protein solution to characterise the likelihood of protein contact air–liquid and solid–liquid interfaces (Koepf et al., 2018).

Our findings show that the dilution of mAb (from 10 to 0.45 mg/mL) still met the sufficient level of surfactant (from 0.2 to 0.009 mg/mL of PS80) to inhibit protein adsorption to interfaces and aggregation (EMA, 2024). According to a few studies (Deechongkit et al., 2009; Garidel et al., 2020), the critical micelle concentration (CMC) of PS80 in water was identified around 0.01 mg/mL, which is lower or equivalent to the PS80 concentrations used in our study (ranging from 0.009 to 0.2 mg/mL). Therefore, even at our lowest PS80 concentration of 0.009 mg/mL, the surfactant is present above its CMC, suggesting that micelle formation is likely sufficient to inhibit protein adsorption to interfaces and aggregation. However, further verification is needed considering variables such as headspace volume in infusion bags, different diluents (e.g., 5 % dextrose), and IV bag materials (e.g., PVC/PO). These approaches may make it possible to lower the concentration of or even to omit surfactants in protein formulations. Formulations with lower concentration of surfactants could be beneficial because surfactants may

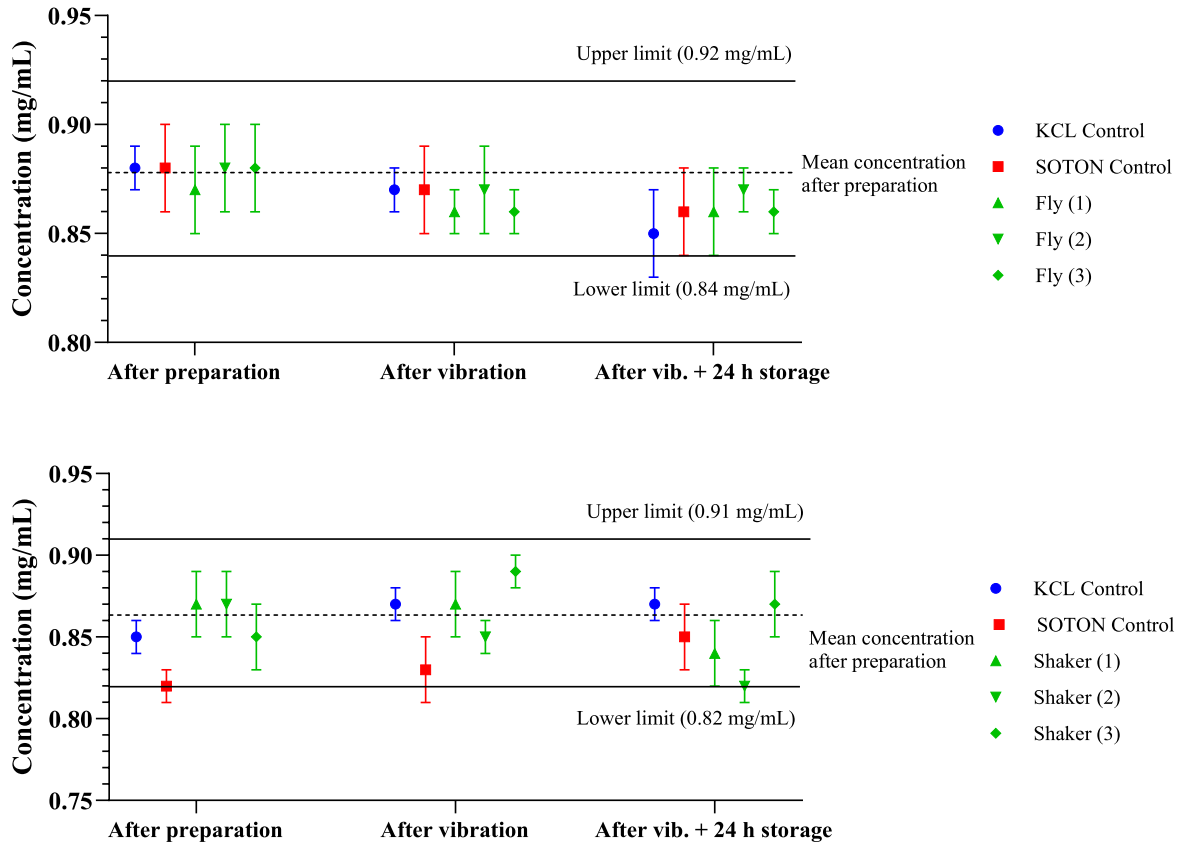

Fig. 14. Concentration of the Nivolumab samples (0.86 mg/mL in 0.9 % w/v NaCl) in the infusions exposed to drone flight (above) and simulated vibration on shaker (below) for 43 min within the three-day test. Data as shown as mean ± SD (n = 3). The upper and lower limits are set by ±5 % variation of mean concentration of all 11 samples.

increase nanometre aggregates as shown in this study and the previous study (Kizuki et al., 2022).

In Study 1, SE-HPLC analysis (Fig. 13) revealed a slight but statistically significant increase in monomer content in two of the three samples exposed to 125 Hz vibration, which persisted after 24-hour storage. The reported monomer variation (≤0.16 %) remains within pharmaceutically acceptable limits and aligns with findings from similar studies, including published work on drone-delivered monoclonal antibodies (Güngören et al., 2024). Besides, this study was intentionally designed to simulate edge-of-failure scenarios, with the test duration of 1 h exceeding typical time at high frequency (125 Hz) to reflect real-world clinical conditions.

Several explanations may account for the apparent monomer increase. For example, vibration-induced fragmentation could generate LMWS that co-elute with buffer components or blend into the chromatographic baseline (Gil & Schrum, 2013). Alternatively, certain aggregation pathways may form soluble oligomers that co-elute with the monomer peak (Roberts, 2014), or adsorption of HMWS/LMWS to infusion bag materials could reduce detectable aggregate levels, resulting in a relative monomer increase. Phase-separated larger aggregates may also settle out of solution, becoming undetectable by SE-HPLC while preserving total protein concentration (Hong et al., 2012).

While the observed 3 nm particle size shift was initially described as "reversible", this lacks direct mechanistic confirmation via other techniques. However, the transient and inconsistent nature of the shift across replicates, combined with the absence of corresponding increases in aggregation or particle counts, suggests no substantive impact on product quality. The authors recognise the importance of incorporating orthogonal techniques in future work to improve mechanistic understanding but emphasise that the current results remain consistent with regulatory expectations and practical application, particularly in ensuring timely and stable delivery of biologics in patient-centred settings.

Future studies may apply SEC-MALS (size exclusion chromatography with multi-angle light scattering) to distinguish true monomeric species from co-eluting aggregates (Some et al., 2019), micro-flow imaging (MFI) or nanoparticle tracking analysis (NTA) to assess subvisible aggregates not captured by SE-HPLC (Telikepalli et al., 2014), and binding assays or functional potency assessments to determine whether these minor variations impact therapeutic activity.

In study 4, the DLS analysis revealed a decrease in the Z-average particle size of Nivolumab by approximately 1.5 nm following vibration exposure. This change exceeds the commonly accepted threshold of 1 nm for size variations in mAbs, as noted by Guyader et al. (2020). This reduction may be attributed to the dissociation of loosely associated oligomers as the monomer dimer equilibrium naturally exists, potentially facilitated by the direct applied airframe frequency in the simulation study. Without adequate protective packaging, such as a cardboard box or shock-absorbing components, mechanical stress from drone vibration could disrupt weak intermolecular interactions, leading

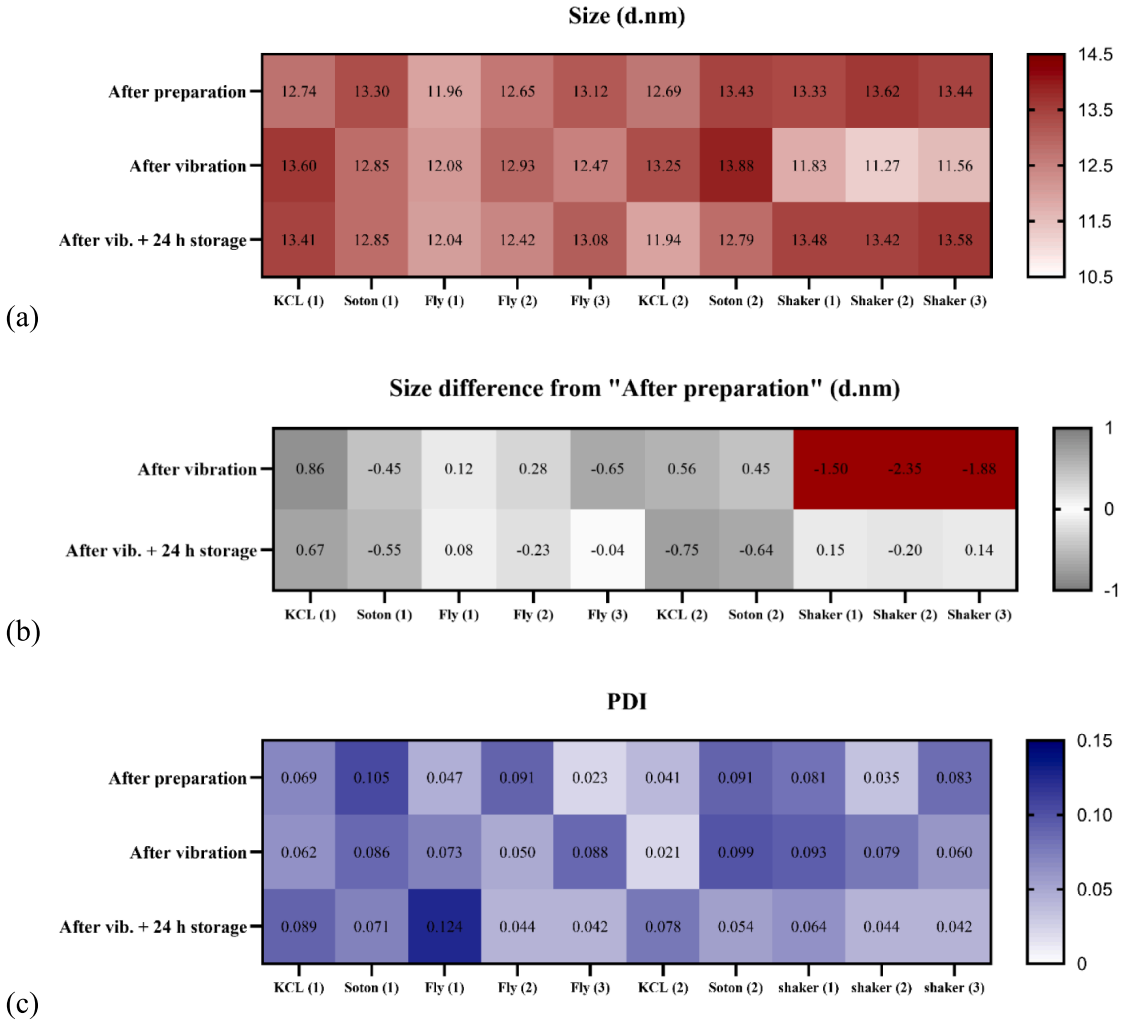

Fig. 15. DLS results of Nivolumab samples (0.86 mg/mL in 0.9 % w/v NaCl) in the infusions exposed to drone flight and simulated vibration on shaker for 43 min within the three-day test. (a) Z-average size (nm). (b) Z-average size difference from "after preparation" measured on Day 1. (c) PDI. Acceptable range: hydrodynamic size variation <1 nm, PDI < 0.3. KCL: the "KCL control" sample, Soton: the "Soton" control sample. The flight trial and shaker replication experiment were completed in different times with two set of samples prepared, so that the control samples have been named as KCL (1) & Soton (1) for fly trial, KCL (2) & Soton (2) for shaker replication.

to a shift toward smaller particle sizes.

Although DLS is widely used for assessing mAb size distribution and aggregation, there is no universally defined regulatory threshold for acceptable size variation in quality control. The International Council for Harmonisation of Technical Requirements for Pharmaceuticals for Human Use (ICH) (1999) and U.S. Food and Drug Administration (FDA) (2018) generally recommend monitoring Z-average and PDI to ensure batch consistency, but specific numerical acceptance criteria, especially for the size changes are typically set by manufacturers based on empirical data and validated through stability studies. In practice, a size change exceeding 1–2 nm is often considered notable for a mAb, particularly if accompanied by increased PDI or emerging aggregation peaks (Nobbmann et al., 2007).

High-accuracy particle counting techniques such as High-Intensity Liquid Particle Counting (HIAC) are more frequently utilized for sub-visible particle detection (Singh et al., 2010). More importantly, HIAC is particularly relevant for regulatory compliance with USP <788> (US Pharmacopoeia, 2016) and European Pharmacopoeia (Ph. Eur.) 2.9.19 (European Pharmacopoeia, 2007), which define limits for subvisible particles in injectable biologics (e.g., ≤6,000 particles/mL for 10–25 μm and ≤ 600 particles/mL for > 25 μm). While DLS provides valuable insights into Z-average particle size and PDI, it is less effective for detecting large aggregates (>1 μm) due to its reliance on intensity-weighted size distribution, which can overemphasize smaller particles (Scherer et al., 2012). The FDA (2015) and ICH Q6B (1999) guidelines also emphasize the importance of complementary techniques, including DLS, HIAC, MFI, and SEC-MALS, to provide a more comprehensive stability profile for therapeutic proteins.

Replicating the vibration conditions of real drone flights in the laboratory offers significant advantages, enabling more extensive sample testing under simulated flight conditions without incurring the cost, risk, and logistical challenges of live flight trials. This approach also facilitates testing over extended flight durations, allowing systems to be future proofed for flights exceeding the capabilities of current drone platforms.

The reported simulation and replication results indicate that no

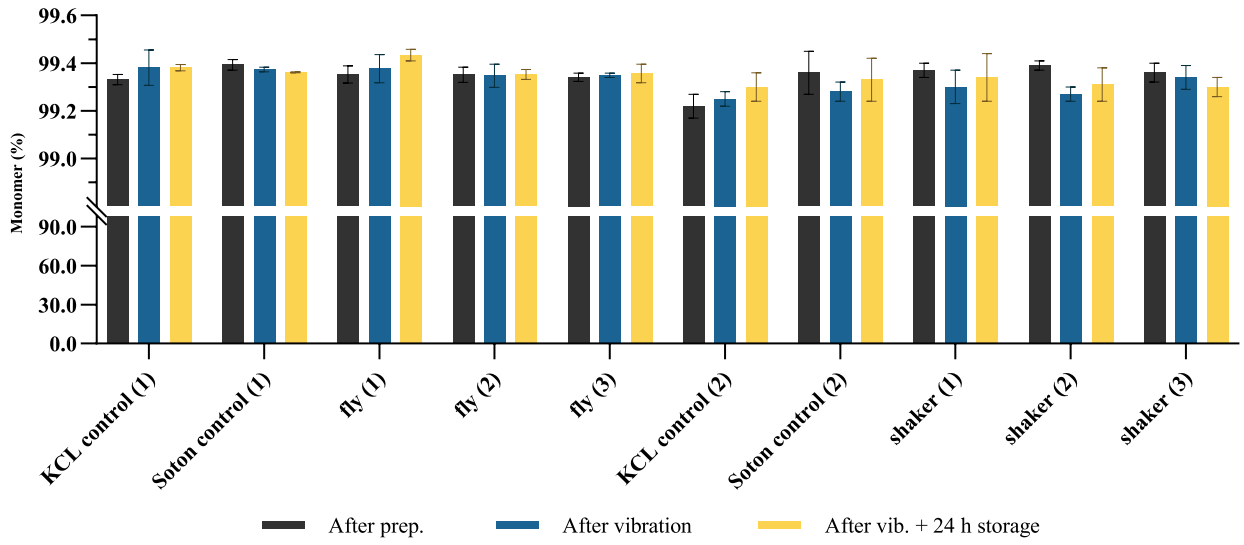

Fig. 16. Monomer content of Nivolumab samples (0.86 mg/mL in 0.9 % w/v NaCl) exposed to drone flight and simulated vibration on shaker for 43 min within the three-day test. Data as shown as mean ± SD (n = 3).

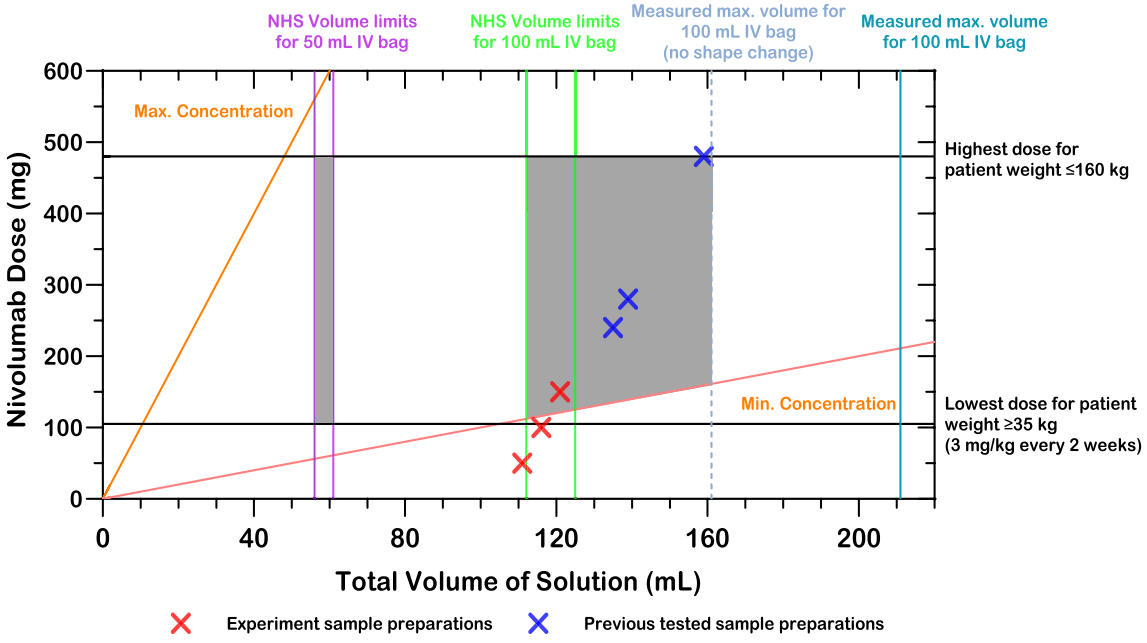

Fig. 17. The volume and dose of Nivolumab preparations in IV bags.

samples tested and reported in this paper within the defined parameters failed to meet the acceptance criteria. ELISA testing would further confirm the stability of Nivolumab towards drone flight. But this efficacy studied is not mandated to show that Good Distribution Practice has been maintained (MHRA, 2017).

Future iterations of this protocol may incorporate sine sweeps, in which the instantaneous frequency varies with time, to more comprehensively cover the total frequency range. Furthermore, the frequency range of the sweep can be tailored to the target range of vibration for any given mode of transport, not limited to 8–200 Hz for a drone.

Additionally, as a failure of Nivolumab stability has not been induced during these trials it may be beneficial to undertake more extreme stress tests to attempt to identify thresholds beyond which failure is likely. This will allow drone providers/stakeholders to compare the vibration profile of their platform to these limits without the need to complete additional trials. This could include a sweep over the full frequency range of the target environment for the maximum achievable magnitude of vibration and long duration.

Consideration of concentration coverage is illustrated in Fig. 17, as infusion volume and mAb dose is tailored to individual patients. The treatment concentration of Nivolumab is 1–10 mg/mL, (NHS England, 2018). To achieve this, the final volume of Nivolumab preparations in 50 mL infusion bags was between 56 and 61 mL and for 100 mL bags between 112 and 125 mL. In clinical practice 100 mL infusion bags are more frequently used and could contain 161 mL solution without shape changed (Fig. 18), with a maximum volume up to 211 mL without

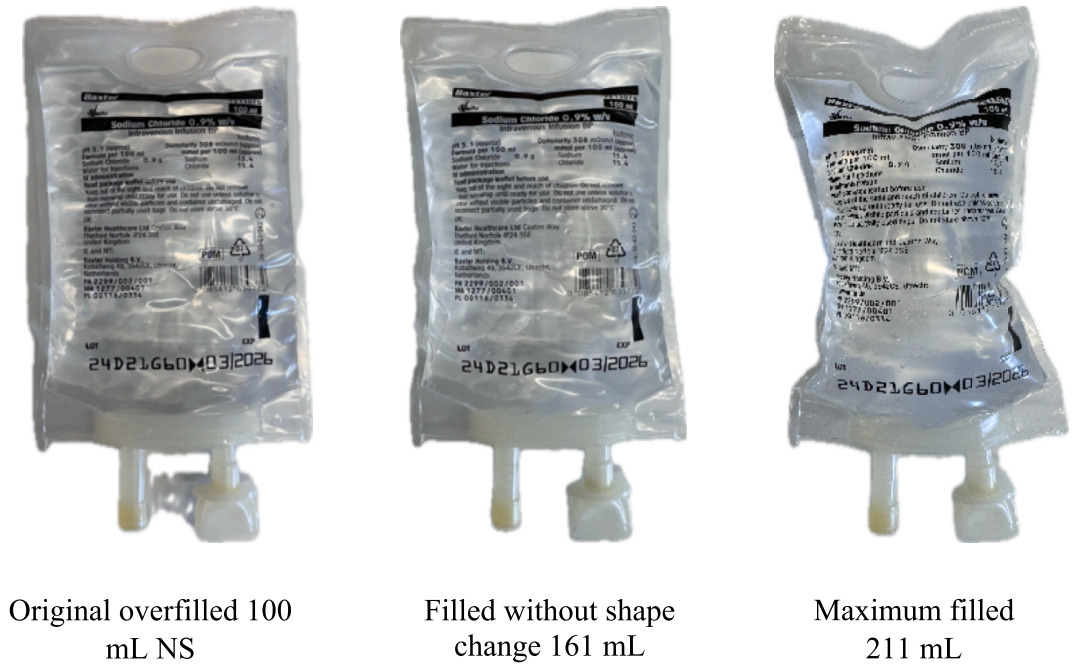

Fig. 18. Baxter 100 mL infusion bag filled with different volume of 0.9 % NaCl.

Table 4
Summary of quality tests results. Green: statistically no difference and within acceptance criteria, Red: out of acceptance criteria, Dark yellow: two samples show statistic differences, light yellow: one sample shows statistic differences.

breaking the bags. The current study investigated 0.45, 0.86 & 1.24 mg/mL in 100 mL IV bags (red cross), which are clinically relevant and are located at the edge of the dosing profile. The aim here was to test samples with the lowest amount of stabilizing surfactant. Clinically nivolumab is most frequently prescribed covering the treatment concentrations 1.07 to 3.52 mg/mL. The blue crosses in Fig. 17 are the previous tested Nivolumab samples prepared but not administered from the Cancer unit at St Mary's Hospital of Isle of Wight NHS, so this orthogonal combination of two sets of samples nicely bracketed the design range of doses and volumes. The authors would have liked to have explored more combinations however due to the expense and availability of the nivolumab concentrate this was not possible.

Additional flight trials would enhance the learnings from this study. For example, "ABA" testing, (store, fly, store), and even using older airframes at the end of their service life to explore Worst-case vibration. This will contribute to the evidence base to support the selection of parameters for the target environment and inform any variation/extension of these parameters.

In all the studies undertaken to date the vibration induced with a shaker has been in the vertical direction only. This is due to the limitation of the available equipment to only produce vibration in one orthogonal direction. The vertical direction was selected as this is most commonly the predominant vertical direction observed during live flight trials. A comparison has been made between the flight recording and the recording of the replication and this shows that the overall resultant RMS vibration of the single axis replication (1.84 g) constitutes 94 % of the flight overall resultant RMS (1.96 g). Future testing could be undertaken to compare the effects when all three orthogonal directions are replicated, for which more specialist equipment would be required.

Considering aviation safety and ethical considerations, it should be noted that mAbs are not classified as dangerous goods under current aviation regulations set by the International Civil Aviation Organization (ICAO) and the International Air Transport Association (IATA), and therefore do not carry a UN Dangerous Goods classification number. Consistent with IATA Packing Instruction 650, the study employed triple-layer, clearly labelled, leak-proof packaging with absorbent and rigid outer containment to ensure compliance with pharmaceutical and aviation standards. As an added precaution, the inclusion of a spill response kit within the drone cargo is recommended. This approach mirrors established practices widely used in the pharmaceutical industry, where biologics and vaccines are routinely transported by air under similar conditions. The authors maintain that these procedures, combined with regulatory adherence and risk mitigation strategies, ensure a high standard of safety to protect the patient, the public and healthcare workers throughout the logistics process.

5. Conclusion

The results revealed all Nivolumab infusions, prepared in NS, were stable after being exposed to simulated drone vibration on the day after; analysis did not show formation of aggregates or measurable losses of protein in solution, with the quality attributes evaluated all within

acceptance criteria. The concluded results have been shown in Table 4. The quality attributes in this study included solution appearance, pH, protein concentration, subvisible particulate matter levels (DLS) and size homogeneity (SE-HPLC).

The infusions were exposed to different frequencies (8/63/125 Hz for 30 mins); duration (60/120/180 mins at 63 Hz) shaking were no different to those of the control infusions that were not exposed to shaking after vibration (day 2) and after 24-hour storage (day 3).

This study obtained positive experimental evidence on quality assurance of Nivolumab infusions at simulated drone transportation vibration conditions. This framework could be useful for other medicine candidates to assist in gaining approvals for drone transportation. However, the vibration profiles of drones would have to be recorded and simulated on an individual basis to satisfy the regulator. There is scope to incorporate flight replication testing into formal protocol for the testing of medicines sensitivity to vibration in addition to the protocol set out in this report. Particularly in the short to medium term flight replication testing may be a suitable method to provide evidence of the safety of specific drone and cargo combinations for overseeing authorities such as the MHRA whilst a formal protocol is being developed and adopted.

CRediT authorship contribution statement

W. Zhu: Writing – review & editing, Writing – original draft, Validation, Resources, Methodology, Investigation, Formal analysis, Data curation, Conceptualization. **K. Theobald:** Writing – review & editing, Writing – original draft, Validation, Resources, Methodology, Investigation, Formal analysis, Data curation, Conceptualization. **M. Tobyn:** Writing – review & editing, Validation, Supervision, Resources, Project administration, Funding acquisition. **P. Courtney:** Writing – review & editing, Supervision, Resources, Project administration, Funding acquisition. **P.G. Royall:** Writing – review & editing, Writing – original draft, Supervision, Project administration, Investigation, Funding acquisition, Formal analysis, Conceptualization. **T. Cherrett:** Writing – review & editing, Supervision, Investigation, Funding acquisition. **T. Waters:** Writing – review & editing, Supervision, Formal analysis, Data curation.

Funding

This study was funded by Solent Transport under the Future Transport Zone 'Drones' project. Additionally, KCL-CSC provided financial support for Wanqing Zhu's PhD project.

Declaration of competing interest

The authors declare the following financial interests/personal relationships which may be considered as potential competing interests: Wanqing Zhu reports financial support was provided by KCL-CSC. Tom Cherrett reports financial support was provided by Future Transport Zone. If there are other authors, they declare that they have no known competing financial interests or personal relationships that could have appeared to influence the work reported in this paper.

Acknowledgement

The authors would like to acknowledge Bristol Myers Squibb (Moreton, UK) for providing the essential Opdivo and the analytical column for this study. Special thanks to Zhi Chen in Drug Product Development (New Jersey, USA) for assistance with the analytical column and valuable insights into the analytical methodology, and to Jonathan Golightly in Clinical Supply (Moreton, UK) for facilitating the arrangement and delivery of the samples. We also extend our gratitude to Erinc Sahin in Drug Product Development (New Jersey, USA) for reviewing the manuscript and providing constructive feedback.

Furthermore, we would like to thank Ans-Mari Bester from St Mary's Hospital, Isle of Wight NHS Trust, for her support in establishing collaborations and for providing valuable insights into patient concerns related to medicine transportation and administration.

We sincerely thank Chemotherapy Production and Dispensing Unit of Guy's Hospital, Guy's and St Thomas' NHS Foundation Trust. Corina Ragazan for aseptic preparation training, and Victoria Fashina for her valuable suggestions and advice. Their support and expertise have been greatly appreciated.

Wanqing Zhu reports financial support was provided by KCL-CSC. Tom Cherrett reports financial support was provided by Future Transport Zone. If there are other authors, they declare that they have no known competing financial interests or personal relationships that could have appeared to influence the work reported in this paper.

Appendix. Summary of quality assessments data.

.

Table A1
UV protein concentration analysis parameters.

Equipment	Perkin Elmer, Lambda 365 UV/Vis Spectrophotometer
Measurement Wavelength	280 nm
Reference Wavelength	360 nm
Blank	Normal Saline
Temperature	25 ℃
Molar extinction coefficient (ϵ)	1.68
Dilution factor	5
Pathlength	1 cm
Cell	PerkinElmer™, 80,631,009

Table A2
DLS analysis parameters.

Equipment	Malvern NanoZS90 ZetaSizer
Material Refractive Index	1.450
Dispersant	Water
Temperature	25 ℃ (equilibrate 30 s)
Measurement Angle	173° Backscatter
Sample Volume	~0.5 mL (1.0–1.5 cm height)
Cell	DTS0012 disposable Cuvettes

Table A3
SE-HPLC analysis parameters.

Equipment	Agilent 1260 s HPLC with UV/Vis detector
Column	Agilent AdvanceBio SEC 300Å guard column, 4.6 × 50 mm, 2.7 μm, PL1580-1301 Agilent AdvanceBio SEC 300Å analytical column, 4.6 × 150 mm, 2.7 μm, PL1580-3301
Container	Fisherbrand™ 2 in 1 Vial Kit, Amber glass, PP screw cap, 11,890,892
Mobile Phase	0.1 mM Potassium phosphate buffer + 0.2 mM Potassium Chloride (pH = 7.0)
Flow rate	0.35 mL/min
Temperature	25 ℃
Injection Volume	5 μL
Detection Wavelength	280 nm (Reference at 360 nm)
Acquisition Time	15 mins

The typical example spectrum of UV (Fig. A1), DLS (Fig. A2) and SE-HPLC (Fig. A3) measurements have been shown below, the KCL control sample (stored at 4 ℃, tested at 25 ℃) in study 2 have been used.

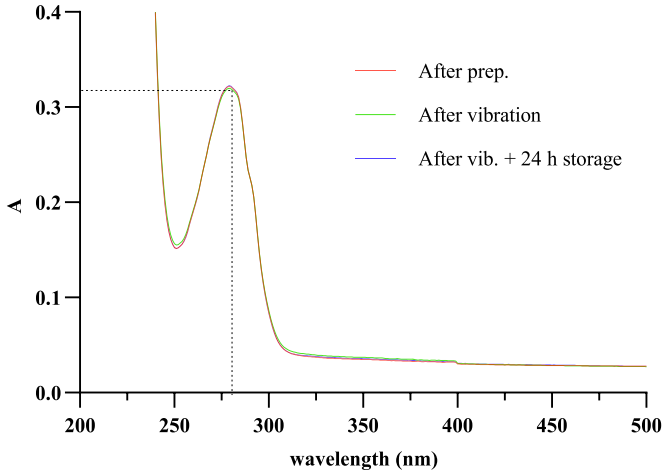

Fig. A1. UV absorbance of Nivolumab 0.86 mg/mL in 0.9 % w/v Sodium Chloride. Absorbance at 280 nm is selected to calculate the concentration.

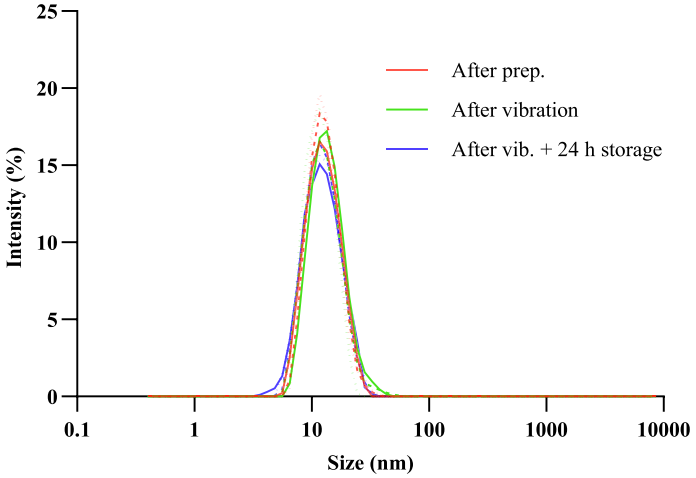

Fig. A2. DLS of Nivolumab 0.91 mg/mL in 0.9 % w/v Sodium Chloride. The line in the same color but different patterns are three different measurements.

Table A4
DLS of Nivolumab 0.91 mg/mL in 0.9 % Sodium Chloride. The line in same colour but different patterns are three different measurements.

Sample	Temperature	Z-average (d.nm)	PDI	Meet criteria?
After Preparation	24.9	12.63	0.083	✓
		12.70	0.088	
		12.16	0.092	
After vibration	25.1	13.24	0.081	✓
		13.31	0.076	
		13.06	0.092	
After vibration + 24 h storage	25.0	13.29	0.089	✓
		13.01	0.105	
		13.24	0.093	

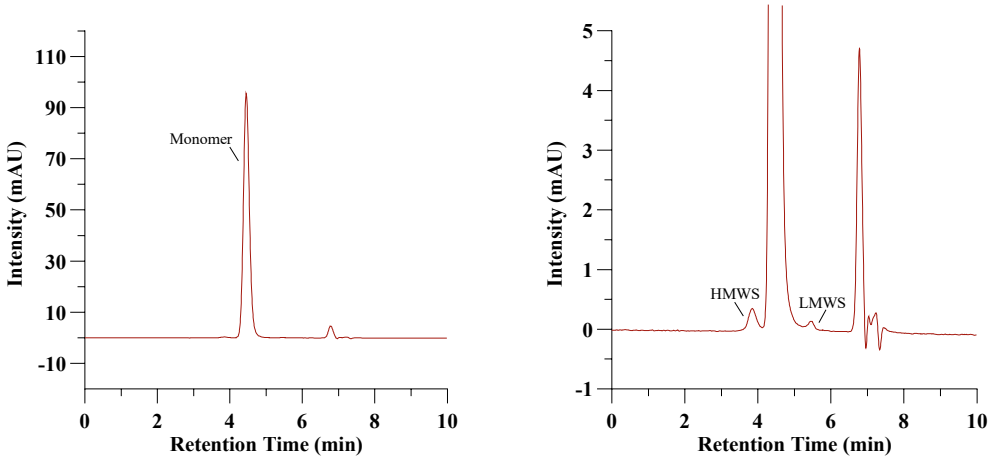

Fig. A3. SE-HPLC elution profile of Nivolumab 0.91 mg/mL in 0.9 % Sodium Chloride.

Table A5
SE-HPLC integration results of Nivolumab 0.91 mg/mL in 0.9 % Sodium Chloride.

Peak	Retention Time	Area	%Area	Height
HMWS	4.145	4.6	0.471	0.898
Monomer	4.854	967.2	98.997	0.67
LMWS	5.403	5.2	0.532	0.151

Data shown for SE-HPLC is the mean ± standard deviation of three measurements, for DLS is the mean of three measurements. All the prepared samples in infusion bags have been analysed for three times. After preparation (day 1), after vibration (day 2), after 24 h storage (day 3).

Table A6
Study 1. Vibration frequency SE-HPLC analysis was performed on the 42 days after preparation because of the column damage, all the other analysis was performed as described above. "*" represents $p < 0.05$.

Infusion	Sample	Appear. /pH at 25.0 °C	Protein Conc. A_{280} (mg/ml)	Subvisible Particles by DLS		SE-HPLC		
				Z-Average (nm)	PDI	HMWS (%)	Monomer (%)	LMWS (%)
KCL control	Preparation	CCS/6.05	0.84 ± 0.02	12.50 ± 0.29	0.088 ± 0.005	0.48 ± 0.02	99.38 ± 0.02	0.14 ± 0.01
	Vibration	CCS/6.07	0.84 ± 0.01	13.20 ± 0.13	0.083 ± 0.009	0.49 ± 0.04	99.39 ± 0.05	0.12 ± 0.01
	24 h Storage	CCS/6.04	0.85 ± 0.02	13.18 ± 0.15	0.096 ± 0.008	0.50 ± 0.04	99.39 ± 0.04	0.11 ± 0.01
Soton control	Preparation	CCS/6.04	0.84 ± 0.01	12.17 ± 0.76	0.063 ± 0.018	0.52 ± 0.02	99.35 ± 0.02	0.13 ± 0.01
	Vibration	CCS/6.03	0.83 ± 0.02	12.80 ± 0.18	0.086 ± 0.018	0.50 ± 0.04	99.39 ± 0.04	0.12 ± 0.01
	24 h Storage	CCS/6.04	0.84 ± 0.02	12.72 ± 0.66	0.091 ± 0.007	0.48 ± 0.01	99.40 ± 0.02	0.12 ± 0.01
Shaker 30 mins 8 Hz ①	Preparation	CCS/6.04	0.84 ± 0.02	12.46 ± 0.87	0.043 ± 0.014	0.53 ± 0.03	99.35 ± 0.03	0.12 ± 0.03
	Vibration	CCS/6.04	0.83 ± 0.02	12.59 ± 0.20	0.102 ± 0.013	0.49 ± 0.03	99.39 ± 0.03	0.12 ± 0.00
	24 h Storage	CCS/6.02	0.84 ± 0.02	12.65 ± 0.86	0.068 ± 0.008	0.52 ± 0.02	99.35 ± 0.06	0.13 ± 0.04
Shaker 30 mins 8 Hz ②	Preparation	CCS/6.04	0.84 ± 0.01	12.65 ± 0.40	0.092 ± 0.013	0.52 ± 0.04	99.32 ± 0.09	0.16 ± 0.05
	Vibration	CCS/6.03	0.84 ± 0.02	12.62 ± 0.62	0.041 ± 0.017	0.48 ± 0.01	99.41 ± 0.00	0.12 ± 0.01
	24 h Storage	CCS/6.07	0.83 ± 0.01	13.48 ± 0.63	0.043 ± 0.006	0.49 ± 0.01	99.40 ± 0.01	0.11 ± 0.01
Shaker 30 mins 8 Hz ③	Preparation	CCS/6.03	0.82 ± 0.02	12.76 ± 0.69	0.046 ±0.005	0.54 ± 0.04	99.34 ± 0.06	0.13 ± 0.02
	Vibration	CCS/6.04	0.81 ± 0.01	12.47 ± 0.78	0.103 ± 0.004	0.51 ± 0.05	99.36 ± 0.06	0.12 ± 0.01
	24 h Storage	CCS/6.09	0.80 ± 0.02	12.95 ± 0.44	0.061 ± 0.003	0.52 ± 0.03	99.36 ± 0.03	0.12 ± 0.01
Shaker 30 mins 63 Hz ①	Preparation	CCS/6.04	0.84 ± 0.01	12.97 ± 0.32	0.034 ± 0.011	0.52 ± 0.02	99.37 ± 0.02	0.11 ± 0.00
	Vibration	CCS/6.00	0.83 ± 0.01	13.16 ± 0.35	0.083 ± 0.008	0.52 ± 0.02	99.34 ± 0.06	0.14 ± 0.04
	24 h Storage	CCS/6.02	0.84 ± 0.01	13.20 ± 0.30	0.091 ± 0.017	0.53 ± 0.05	99.35 ± 0.07	0.12 ± 0.02
Shaker 30 mins 63 Hz ②	Preparation	CCS/6.02	0.83 ± 0.02	12.27 ± 0.22	0.031 ± 0.015	0.55 ± 0.04	99.33 ± 0.02	0.12 ± 0.01
	Vibration	CCS/6.06	0.81 ± 0.02	12.32 ± 0.33	0.094 ± 0.011	0.52 ± 0.04	99.36 ± 0.05	0.12 ± 0.00
	24 h Storage	CCS/6.03	0.82 ± 0.02	12.82 ± 0.70	0.067 ± 0.014	0.54 ± 0.03	99.35 ± 0.03	0.11 ± 0.02
Shaker 30 mins 63 Hz ③	Preparation	CCS/6.02	0.81 ± 0.02	12.37 ± 0.70	0.059 ± 0.013	0.55 ± 0.04	99.29 ± 0.02	0.16 ± 0.06
	Vibration	CCS/6.01	0.79 ± 0.03	12.72 ± 0.56	0.065 ± 0.014	0.53 ± 0.03	99.36 ± 0.03	0.11 ± 0.01
	24 h Storage	CCS/6.06	0.82 ± 0.01	13.15 ± 0.22	0.034 ± 0.006	0.53 ± 0.04	99.35 ± 0.02	0.12 ± 0.00
Shaker 30 mins 125 Hz ①	Preparation	CCS/6.04	0.83 ± 0.01	11.71 ± 0.20	0.034 ± 0.017	0.56 ± 0.02	99.23 ± 0.03	0.21 ± 0.04
	Vibration	CCS/6.03	0.80 ± 0.02	12.81 ± 0.44	0.083 ± 0.015	**0.50 ± 0.01***	**99.39 ± 0.01***	**0.12 ± 0.00***
	24 h Storage	CCS/6.01	0.81 ± 0.02	12.26 ± 0.51	0.044 ± 0.009	**0.51 ± 0.02***	**99.37 ± 0.03***	**0.13 ± 0.01***
Shaker 30 mins 125 Hz ②	Preparation	CCS/6.07	0.83 ± 0.02	11.92 ± 0.18	0.072 ± 0.006	0.57 ± 0.06	99.24 ± 0.10	0.18 ± 0.08
	Vibration	CCS/6.02	0.81 ± 0.02	12.10 ± 0.52	0.062 ± 0.013	**0.49 ± 0.01***	**99.40 ± 0.01***	**0.12 ± 0.01***
	24 h Storage	CCS/6.03	0.82 ± 0.01	11.89 ± 0.91	0.108 ± 0.012	**0.52 ± 0.02***	**99.36 ± 0.02***	**0.12 ± 0.00***
Shaker 30 mins 125 Hz ③	Preparation	CCS/6.02	0.85 ± 0.01	12.43 ± 0.58	0.045 ± 0.011	0.55 ± 0.05	99.29 ± 0.03	0.15 ± 0.07
	Vibration	CCS/6.04	0.85 ± 0.02	12.53 ± 0.62	0.072 ± 0.018	0.53 ± 0.04	99.35 ± 0.03	0.12 ± 0.00
	24 h Storage	CCS/6.06	0.84 ± 0.01	12.28 ± 0.59	0.039 ± 0.015	0.54 ± 0.01	99.33 ± 0.01	0.13 ± 0.00

Table A7
Study 2. Vibration duration.

Infusion	Time of test (after)	Appear. /pH at 25.0 ℃	Protein Conc. A_{280} (mg/ml)	Subvisible Particles by DLS		SE-HPLC		
				Z-Average (nm)	PDI	HMWS (%)	Monomer (%)	LMWS (%)
KCL control	Preparation	CCS/6.11	0.81 ± 0.02	12.04 ± 0.35	0.069 ± 0.011	0.52 ± 0.02	99.32 ± 0.06	0.16 ± 0.04
	Vibration	CCS/6.14	0.82 ± 0.01	12.32 ± 0.55	0.023 ± 0.009	0.48 ± 0.03	99.39 ± 0.03	0.13 ± 0.02
	24 h Storage	CCS/6.15	0.83 ± 0.02	12.62 ± 0.32	0.046 ± 0.014	0.53 ± 0.05	99.31 ± 0.09	0.16 ± 0.04
Soton control	Preparation	CCS/6.12	0.82 ± 0.02	12.49 ± 0.44	0.039 ± 0.003	0.52 ± 0.01	99.31 ± 0.07	0.17 ± 0.07
	Vibration	CCS/6.16	0.83 ± 0.02	12.60 ± 0.58	0.083 ± 0.020	0.50 ± 0.07	99.35 ± 0.07	0.15 ± 0.01
	24 h Storage	CCS/6.15	0.84 ± 0.02	12.72 ± 0.66	0.091 ± 0.017	0.49 ± 0.02	99.37 ± 0.02	0.13 ± 0.02
Shaker 63 Hz 60 mins ①	Preparation	CCS/6.15	0.82 ± 0.02	12.69 ± 0.08	0.072 ± 0.017	0.49 ± 0.00	99.41 ± 0.01	0.10 ± 0.00
	Vibration	CCS/6.17	0.83 ± 0.01	12.81 ± 0.48	0.092 ±0.008	0.48 ± 0.01	99.41 ± 0.02	0.11 ± 0.01
	24 h Storage	CCS/6.14	0.84 ± 0.02	12.65 ± 0.86	0.068 ± 0.008	0.51 ± 0.05	99.33 ± 0.10	0.16 ± 0.05
Shaker 63 Hz 60 mins ②	Preparation	CCS/6.14	0.84 ± 0.01	12.62 ± 0.62	0.041 ± 0.007	0.49 ± 0.02	99.41 ± 0.02	0.10 ± 0.01
	Vibration	CCS/6.18	0.85 ± 0.02	12.70 ± 0.76	0.074 ± 0.004	0.50 ± 0.04	99.38 ± 0.06	0.12 ± 0.02
	24 h Storage	CCS/6.11	0.84 ± 0.02	13.48 ± 0.63	0.043 ± 0.006	0.50 ± 0.02	99.39 ± 0.03	0.11 ± 0.02
Shaker 63 Hz 60 mins ③	Preparation	CCS/6.10	0.85 ± 0.03	12.35 ± 0.41	0.063 ±0.005	0.51 ± 0.03	99.36 ± 0.07	0.13 ± 0.04
	Vibration	CCS/6.12	0.84 ± 0.02	12.92 ± 0.33	0.045 ± 0.015	0.52 ± 0.04	99.37 ± 0.04	0.10 ± 0.00
	24 h Storage	CCS/6.13	0.84 ± 0.03	12.95 ± 0.44	0.061 ± 0.003	0.57 ± 0.02	99.29 ± 0.04	0.14 ± 0.01
63 Hz 120 mins ①	Preparation	CCS/6.17	0.79 ± 0.01	12.41 ± 0.16	0.062 ± 0.014	0.54 ± 0.03	99.29 ± 0.07	0.17 ± 0.04
	Vibration	CCS/6.18	0.78 ± 0.01	12.71 ± 0.12	0.073 ± 0.003	0.52 ± 0.07	99.38 ± 0.08	0.10 ± 0.01
	24 h Storage	CCS/6.11	0.80 ± 0.02	13.20 ± 0.30	0.091 ± 0.017	0.56 ± 0.05	99.30 ± 0.05	0.13 ± 0.01
63 Hz 120 mins ②	Preparation	CCS/6.16	0.84 ± 0.02	12.94 ± 0.76	0.096 ± 0.013	0.52 ± 0.01	99.33 ± 0.08	0.15 ± 0.08
	Vibration	CCS/6.12	0.85 ± 0.01	13.60 ± 0.82	0.130 ± 0.047	0.55 ± 0.02	99.29 ± 0.07	0.16 ± 0.05
	24 h Storage	CCS/6.15	0.84 ± 0.02	12.82 ± 0.70	0.067 ± 0.014	0.55 ± 0.03	99.32 ± 0.03	0.13 ± 0.02
63 Hz 120 mins ③	Preparation	CCS/6.12	0.82 ± 0.02	12.24 ± 0.28	0.064 ± 0.002	0.50 ± 0.03	99.37 ± 0.07	0.13 ± 0.04
	Vibration	CCS/6.10	0.81 ± 0.03	13.22 ± 0.86	0.073 ± 0.019	0.57 ± 0.03	99.33 ± 0.04	0.10 ± 0.01
	24 h Storage	CCS/6.15	0.82 ± 0.02	13.15 ± 0.22	0.034 ± 0.006	0.58 ± 0.05	99.29 ± 0.07	0.13 ± 0.02
63 Hz 180 mins ①	Preparation	CCS/6.14	0.84 ± 0.02	12.20 ± 0.66	0.117 ± 0.036	0.51 ± 0.03	99.38 ± 0.03	0.11 ± 0.01
	Vibration	CCS/6.16	0.84 ± 0.01	12.69 ± 0.60	0.081 ± 0.003	0.49 ± 0.08	99.41 ± 0.10	0.11 ± 0.02
	24 h Storage	CCS/6.17	0.83 ± 0.02	12.26 ± 0.51	0.044 ± 0.009	0.51 ± 0.02	99.36 ± 0.01	0.13 ± 0.02
63 Hz 180 mins ②	Preparation	CCS/6.14	0.85 ± 0.02	13.05 ± 0.34	0.082 ± 0.016	0.54 ± 0.01	99.31 ± 0.08	0.15 ± 0.07
	Vibration	CCS/6.16	0.86 ± 0.01	13.38 ± 0.84	0.108 ± 0.013	0.51 ± 0.01	99.38 ± 0.01	0.10 ± 0.00
	24 h Storage	CCS/6.12	0.86 ± 0.01	11.89 ± 0.91	0.093 ± 0.008	0.56 ± 0.02	99.31 ± 0.02	0.12 ± 0.02
63 Hz 180 mins ③	Preparation	CCS/6.11	0.87 ± 0.01	12.28 ± 0.10	0.069 ± 0.011	0.55 ± 0.03	99.32 ± 0.03	0.13 ± 0.05
	Vibration	CCS/6.09	0.86 ± 0.02	12.53 ± 0.62	0.072 ± 0.018	0.53 ± 0.01	99.37 ± 0.02	0.10 ± 0.01
	24 h Storage	CCS/6.12	0.84 ± 0.02	12.78 ± 0.81	0.058 ± 0.008	0.59 ± 0.04	99.28 ± 0.02	0.13 ± 0.02

Table A8
Study 3: Concentration.

Infusion	Time of test (after)	Appear. /pH at 25.0 ℃	Protein Conc. A_{280} (mg/ml)	Subvisible Particles by DLS		SE-HPLC		
				Z-Average (nm)	PDI	HMWS (%)	Monomer (%)	LMWS (%)
KCL control 0.45 mg/mL	Preparation	CCS/6.18	0.46 ± 0.02	12.68 ± 0.61	0.082 ± 0.007	0.51 ± 0.01	99.28 ± 0.02	0.21 ± 0.00
	Vibration	CCS/6.14	0.47 ± 0.01	12.57 ± 0.20	0.068 ± 0.006	0.53 ± 0.01	99.26 ± 0.01	0.20 ± 0.00
	24 h Storage	CCS/6.17	0.48 ± 0.02	12.91 ± 0.39	0.075 ± 0.006	0.53 ± 0.02	99.26 ± 0.02	0.21 ± 0.01
Soton control 0.45 mg/mL	Preparation	CCS/6.12	0.46 ± 0.01	12.61 ± 0.44	0.053 ± 0.015	0.50 ± 0.02	99.30 ± 0.01	0.20 ± 0.03
	Vibration	CCS/6.18	0.48 ± 0.02	12.70 ± 0.38	0.116 ± 0.018	0.52 ± 0.03	99.28 ± 0.03	0.21 ± 0.00
	24 h Storage	CCS/6.18	0.48 ± 0.02	12.22 ± 0.57	0.091 ± 0.007	0.53 ± 0.02	99.27 ± 0.03	0.20 ± 0.01
Shaker 63 Hz 60 mins ① 0.45 mg/mL	Preparation	CCS/6.16	0.46 ± 0.02	13.30 ± 0.45	0.094 ± 0.002	0.53 ± 0.03	99.27 ± 0.02	0.20 ± 0.01
	Vibration	CCS/6.15	0.49 ± 0.02	12.65 ± 0.46	0.074 ±0.004	0.55 ± 0.00	99.25 ± 0.01	0.20 ± 0.01
	24 h Storage	CCS/6.16	0.49 ± 0.02	12.98 ± 0.89	0.065 ± 0.007	0.53 ± 0.01	99.29 ± 0.01	0.19 ± 0.01
Shaker 63 Hz 60 mins ②0.45 mg/mL	Preparation	CCS/6.14	0.46 ± 0.01	12.46 ± 0.89	0.075 ± 0.013	0.53 ± 0.02	99.29 ± 0.02	0.18 ± 0.01
	Vibration	CCS/6.13	0.49 ± 0.02	13.17 ± 0.18	0.085 ± 0.021	0.55 ± 0.02	99.25 ± 0.02	0.20 ± 0.02
	24 h Storage	CCS/6.14	0.47 ± 0.01	12.51 ± 0.65	0.148 ± 0.021	0.55 ± 0.01	99.29 ± 0.01	0.16 ± 0.03
Shaker 63 Hz 60 mins ③0.45 mg/mL	Preparation	CCS/6.12	0.46 ± 0.02	12.49 ± 0.39	0.051 ± 0.023	0.55 ± 0.05	99.26 ± 0.05	0.19 ± 0.00
	Vibration	CCS/6.13	0.47 ± 0.01	12.61 ± 0.23	0.082 ± 0.012	0.56 ± 0.02	99.23 ± 0.01	0.20 ± 0.00
	24 h Storage	CCS/6.11	0.48 ± 0.02	13.21 ± 0.45	0.069 ± 0.023	0.54 ± 0.00	99.31 ± 0.01	0.15 ± 0.01
KCL control 0.86 mg/mL	Preparation	CCS/6.17	0.85 ± 0.02	12.22 ± 0.12	0.066 ± 0.008	0.55 ± 0.04	99.29 ± 0.05	0.16 ± 0.02
	Vibration	CCS/6.19	0.85 ± 0.02	12.39 ± 0.54	0.066 ± 0.010	0.52 ± 0.02	99.30 ± 0.02	0.18 ± 0.02
	24 h Storage	CCS/6.18	0.84 ± 0.02	12.30 ± 0.63	0.067 ± 0.013	0.52 ± 0.01	99.33 ± 0.01	0.16 ± 0.00
Soton control 0.86 mg/mL	Preparation	CCS/6.18	0.86 ± 0.02	13.17 ± 0.61	0.091 ± 0.012	0.56 ± 0.03	99.27 ± 0.04	0.17 ± 0.01
	Vibration	CCS/6.12	0.87 ± 0.02	13.12 ± 0.19	0.089 ± 0.018	0.54 ± 0.04	99.29 ± 0.04	0.17 ± 0.01
	24 h Storage	CCS/6.17	0.87 ± 0.02	13.09 ± 0.33	0.044 ± 0.003	0.53 ± 0.00	99.30 ± 0.01	0.17 ± 0.01
Shaker 63 Hz 60 mins ① 0.86 mg/mL	Preparation	CCS/6.15	0.86 ± 0.01	13.18 ± 0.11	0.043 ± 0.019	0.53 ± 0.05	99.31 ± 0.06	0.16 ± 0.01
	Vibration	CCS/6.16	0.87 ± 0.01	13.47 ± 0.62	0.064 ± 0.008	0.54 ± 0.04	99.26 ± 0.04	0.20 ± 0.01
	24 h Storage	CCS/6.15	0.88 ± 0.01	12.68 ± 0.78	0.071 ± 0.012	0.56 ± 0.04	99.28 ± 0.04	0.16 ± 0.00
Shaker 63 Hz 60 mins ② 0.86 mg/mL	Preparation	CCS/6.16	0.86 ± 0.02	13.16 ± 0.15	0.094 ± 0.017	0.50 ± 0.04	99.34 ± 0.05	0.15 ± 0.01
	Vibration	CCS/6.14	0.87 ± 0.02	12.75 ± 0.85	0.079 ± 0.021	0.53 ± 0.01	99.29 ± 0.02	0.19 ± 0.00
	24 h Storage	CCS/6.17	0.87 ± 0.02	13.28 ± 0.89	0.081 ± 0.020	0.55 ± 0.02	99.29 ± 0.02	0.16 ± 0.01
Shaker 63 Hz 60 mins ③ 0.86 mg/mL	Preparation	CCS/6.17	0.88 ± 0.02	12.88 ± 0.33	0.093 ± 0.016	0.51 ± 0.04	99.31 ± 0.03	0.18 ± 0.02
	Vibration	CCS/6.13	0.86 ± 0.03	12.62 ± 0.24	0.057 ± 0.018	0.53 ± 0.01	99.30 ± 0.01	0.17 ± 0.01
	24 h Storage	CCS/6.14	0.87 ± 0.01	13.15 ± 0.22	0.034 ± 0.006	0.54 ± 0.02	99.29 ± 0.02	0.17 ± 0.00
KCL control 1.24 mg/mL	Preparation	CCS/6.12	1.19 ± 0.02	12.47 ± 0.51	0.045 ± 0.015	0.54 ± 0.02	99.30 ± 0.01	0.16 ± 0.00
	Vibration	CCS/6.16	1.18 ± 0.02	12.63 ± 0.77	0.122 ± 0.049	0.52 ± 0.02	99.33 ± 0.01	0.16 ± 0.01
	24 h Storage	CCS/6.13	1.20 ± 0.02	12.85 ± 0.34	0.087 ± 0.012	0.51 ± 0.01	99.33 ± 0.01	0.16 ± 0.00
Soton control 1.24 mg/mL	Preparation	CCS/6.11	1.20 ± 0.02	12.73 ± 0.40	0.097 ± 0.019	0.54 ± 0.02	99.30 ± 0.02	0.16 ± 0.01
	Vibration	CCS/6.10	1.20 ± 0.03	12.56 ± 0.61	0.052 ± 0.008	0.53 ± 0.01	99.32 ± 0.02	0.16 ± 0.00
	24 h Storage	CCS/6.11	1.21 ± 0.02	12.41 ± 0.31	0.058 ± 0.002	0.52 ± 0.01	99.32 ± 0.01	0.16 ± 0.00
Shaker 63 Hz 60 mins ① 1.24 mg/mL	Preparation	CCS/6.12	1.20 ± 0.01	12.95 ± 0.54	0.108 ± 0.027	0.54 ± 0.02	99.31 ± 0.02	0.16 ± 0.00
	Vibration	CCS/6.12	1.22 ± 0.02	12.59 ± 0.44	0.078 ± 0.006	0.52 ± 0.03	99.32 ± 0.03	0.16 ± 0.00
	24 h Storage	CCS/6.15	1.20 ± 0.02	12.53 ± 0.50	0.064 ± 0.013	0.53 ± 0.02	99.32 ± 0.02	0.15 ± 0.01
Shaker 63 Hz 60 mins ② 1.24 mg/mL	Preparation	CCS/6.14	1.20 ± 0.02	12.75 ± 0.30	0.085 ± 0.012	0.54 ± 0.04	99.29 ± 0.04	0.17 ± 0.00
	Vibration	CCS/6.17	1.22 ± 0.02	12.55 ± 0.66	0.063 ± 0.006	0.54 ± 0.01	99.29 ± 0.01	0.16 ± 0.02
	24 h Storage	CCS/6.13	1.22 ± 0.01	11.89 ± 0.91	0.156 ± 0.028	0.53 ± 0.03	99.32 ± 0.03	0.16 ± 0.00
Shaker 63 Hz 60 mins ③ 1.24 mg/mL	Preparation	CCS/6.12	1.21 ± 0.01	12.25 ± 0.71	0.084 ± 0.009	0.54 ± 0.04	99.30 ± 0.04	0.17 ± 0.00
	Vibration	CCS/6.13	1.22 ± 0.02	12.55 ± 0.93	0.073 ± 0.011	0.54 ± 0.01	99.30 ± 0.01	0.16 ± 0.01
	24 h Storage	CCS/6.14	1.21 ± 0.01	11.99 ± 0.83	0.078 ± 0.015	0.52 ± 0.03	99.32 ± 0.02	0.16 ± 0.01

Table A9
Study 4: Drone flight trial.

Infusion	Sample	Appear. /pH at 25.0 ℃	Protein Conc. A_{280} (mg/ml)	Subvisible Particles by DLS		SE-HPLC		
				Z-Average (nm)	PDI	HMWS (%)	Monomer (%)	LMWS (%)
KCL control	Preparation	CCS/5.87	0.88 ± 0.01	12.74 ± 0.20	0.069 ± 0.012	0.57 ± 0.02	99.33 ± 0.02	0.10 ± 0.01
	Vibration	CCS/5.89	0.87 ± 0.01	13.60 ± 0.86	0.062 ± 0.023	0.53 ± 0.06	99.38 ± 0.07	0.09 ± 0.02
	24 h Storage	CCS/5.87	0.85 ± 0.02	13.41 ± 0.60	0.089 ± 0.027	0.55 ± 0.01	99.38 ± 0.01	0.07 ± 0.00
Soton control	Preparation	CCS/5.87	0.88 ± 0.02	13.30 ± 0.76	0.105 ± 0.031	0.53 ± 0.02	99.39 ± 0.02	0.08 ± 0.00
	Vibration	CCS/5.90	0.86 ± 0.02	12.85 ± 0.18	0.086 ± 0.018	0.55 ± 0.01	99.37 ± 0.01	0.08 ± 0.01
	24 h Storage	CCS/5.90	0.86 ± 0.02	12.85 ± 0.38	0.071 ± 0.022	0.55 ± 0.01	99.36 ± 0.02	0.09 ± 0.01
fly ①	Preparation	CCS/5.85	0.87 ± 0.02	11.96 ± 0.57	0.047 ± 0.013	0.55 ± 0.04	99.35 ± 0.03	0.10 ± 0.01
	Vibration	CCS/5.87	0.86 ± 0.01	12.08 ± 0.41	0.073 ± 0.024	0.53 ± 0.04	99.38 ± 0.06	0.09 ± 0.01
	24 h Storage	CCS/5.87	0.86 ± 0.02	12.04 ± 0.17	0.124 ± 0.035	0.50 ± 0.01	99.43 ± 0.02	0.08 ± 0.01
fly ②	Preparation	CCS/5.86	0.88 ± 0.02	12.65 ± 0.40	0.091 ± 0.014	0.56 ± 0.03	99.35 ± 0.03	0.09 ± 0.01
	Vibration	CCS/5.87	0.87 ± 0.02	12.93 ± 0.25	0.050 ± 0.009	0.57 ± 0.02	99.35 ± 0.05	0.08 ± 0.01
	24 h Storage	CCS/5.90	0.87 ± 0.01	12.42 ± 0.58	0.044 ± 0.011	0.57 ± 0.02	99.35 ± 0.02	0.08 ± 0.01
fly ③	Preparation	CCS/5.88	0.88 ± 0.02	13.12 ± 0.72	0.023 ± 0.007	0.56 ± 0.04	99.34 ± 0.02	0.10 ± 0.02
	Vibration	CCS/5.88	0.86 ± 0.01	12.47 ± 0.56	0.088 ± 0.018	0.57 ± 0.01	99.35 ± 0.01	0.08 ± 0.01
	24 h Storage	CCS/5.89	0.86 ± 0.01	13.08 ± 0.08	0.042 ± 0.012	0.55 ± 0.04	99.36 ± 0.04	0.09 ± 0.00

Table A10
Study 4: shaker simulation.

Infusion	Sample	Appear. /pH at 25.0 ℃	Protein Conc. A_{280} (mg/ml)	Subvisible Particles by DLS		SE-HPLC		
				Z-Average (nm)	PDI	HMWS (%)	Monomer (%)	LMWS (%)
KCL control	Preparation	CCS/5.93	0.85 ± 0.01	12.69 ± 0.39	0.041 ± 0.014	0.55 ± 0.02	98.92 ± 0.05	0.53 ± 0.03
	Vibration	CCS/6.08	0.87 ± 0.01	13.25 ± 0.56	0.021 ± 0.009	0.49 ± 0.01	98.85 ± 0.03	0.66 ± 0.04
	24 h Storage	CCS/5.92	0.87 ± 0.01	11.94 ± 0.20	0.078 ± 0.021	0.51 ± 0.02	98.90 ± 0.06	0.59 ± 0.05
	Preparation	CCS/5.89	0.81 ± 0.01	13.43 ± 0.63	0.091 ± 0.032	0.61 ± 0.10	98.86 ± 0.09	0.53 ± 0.02
Soton control	Vibration	CCS/5.99	0.83 ± 0.02	13.88 ± 0.47	0.099 ± 0.012	0.53 ± 0.02	98.88 ± 0.04	0.59 ± 0.05
	24 h Storage	CCS/5.87	0.84 ± 0.02	12.79 ± 0.43	0.054 ± 0.007	0.57 ± 0.03	98.83 ± 0.09	0.60 ± 0.07
Shaker ①	Preparation	CCS/5.91	0.87 ± 0.02	14.33 ± 0.65	0.081 ± 0.021	0.52 ± 0.04	98.97 ± 0.03	0.51 ± 0.02
	Vibration	CCS/5.93	0.87 ± 0.02	**11.83 ± 0.16**	0.093 ± 0.017	0.51 ± 0.02	98.90 ± 0.07	0.59 ± 0.06
	24 h Storage	CCS/5.92	0.84 ± 0.02	13.48 ± 0.17	0.124 ± 0.015	0.48 ± 0.02	98.94 ± 0.10*	0.58 ± 0.08
Shaker ②	Preparation	CCS/5.92	0.87 ± 0.02	14.62 ± 0.07	0.085 ± 0.002	0.51 ± 0.02	98.99 ± 0.02	0.50 ± 0.01
	Vibration	CCS/5.96	0.84 ± 0.01	**11.27 ± 0.46**	0.079 ± 0.023	0.49 ± 0.02	98.87 ± 0.02	0.64 ± 0.03
	24 h Storage	CCS/5.93	0.82 ± 0.01	13.42 ± 0.58	0.144 ± 0.011	0.45 ± 0.02	98.91 ± 0.07	0.65 ± 0.07
Shaker ③	Preparation	CCS/5.91	0.85 ± 0.02	14.44 ± 0.64	0.083 ±0.027	0.51 ± 0.01	98.96 ± 0.04	0.53 ± 0.03
	Vibration	CCS/5.90	0.89 ± 0.01	**11.56 ± 0.70**	0.060 ± 0.028	0.48 ± 0.01	99.94 ± 0.05	0.58 ± 0.05
	24 h Storage	CCS/5.95	0.87 ± 0.02	13.58 ± 0.08	0.142 ± 0.012	0.46 ± 0.03	98.90 ± 0.04	0.63 ± 0.06

Data availability

Data will be made available on request.

References

APS, 2023. APS 400 ELECTRO-SEIS® | Technical datasheet. APS. https://www.apsdynamics.com/en/products/details/vibration-exciter/aps-400.html?file=files/spektra_relaunch/inhalte/produktgruppen/datenblaetter/APS_400_Data_Sheet_en.pdf.

Baxter, 2024. Product Catalog. Baxter.com. https://ecatalog.baxter.com/ecatalog/loadproduct.html?cid=20016&lid=10001&hid=20001&loadroot=true&categoryId=&pid=821856.

BMS, 2024. OPDIVO 10 mg/mL concentrate for solution for infusion - Summary of Product Characteristics (SmPC) - (emc). Www.medicines.org.uk. https://www.medicines.org.uk/emc/product/6888/smpc.

Cohrs, M., Clottens, N., Ramaut, P., Braeckmans, K., Smedt, S.D., Bauters, T., Svilenov, H. L., 2024. Impact of pneumatic tube transportation on the aggregation of monoclonal antibodies in clinical practice, 106952–106952 Eur. J. Pharm. Sci.. https://doi.org/10.1016/j.ejps.2024.106952.

Dasnoy, S., Illartin, M., Queffelec, J., Nkunku, A., Peerboom, C., 2024. Combined effect of shaking orbit and vial orientation on the agitation-induced aggregation of proteins. J. Pharm. Sci. 113 (3), 669–679. https://doi.org/10.1016/j.xphs.2023.08.016.

Deechongkit, S., Wen, J., Narhi, L.O., Jiang, Y., Park, S.S., Kim, J., Kerwin, B.A., 2009. Physical and biophysical effects of polysorbate 20 and 80 on darbepoetin alfa. J. Pharm. Sci. 98 (9), 3200–3217. https://doi.org/10.1002/jps.21740.

EMA, 2024. ANNEX I SUMMARY OF PRODUCT CHARACTERISTICS. https://www.ema.europa.eu/en/documents/product-information/opdivo-epar-product-information_en.pdf.

European Pharmacopoeia, 2007. 2.9.19. Particulate contamination: sub-visible particles. http://uspbpep.com/ep60/2.9.19.%20particulate%20contamination-%20sub-visible%20particles%2020919e.pdf.

Falke, S., Betzel, C., 2019. Dynamic Light Scattering (DLS). Radiat. Bioanal. 8, 173–193. https://doi.org/10.1007/978-3-030-28247-9_6.
FDA, 2015. Analytical Procedures and Methods Validation for Drugs and Biologics Guidance for Industry. https://www.fda.gov/files/drugs/published/Analytical-Procedures-and-Methods-Validation-for-Drugs-and-Biologics.pdf?utm_source=chatgpt.com.
FDA, 2018. Bioanalytical Method Validation Guidance for Industry. https://www.fda.gov/media/70858/download.
Fleischman, M.L., Chung, J., Paul, E.P., Lewus, R.A., 2017. Shipping-induced aggregation in therapeutic antibodies: utilization of a scale-down model to assess degradation in monoclonal antibodies. J. Pharm. Sci. 106 (4), 994–1000. https://doi.org/10.1016/j.xphs.2016.11.021.
Garidel, P., Blech, M., Buske, J., Blume, A., 2020. Surface tension and self-association properties of aqueous polysorbate 20 HP and 80 HP solutions: insights into protein stabilisation mechanisms. J. Pharm. Innov. 16 (4), 726–734. https://doi.org/10.1007/s12247-020-09488-4.
Gerhardt, A., Mcgraw, N.R., Schwartz, D.K., Bee, J.S., Carpenter, J.F., Randolph, T.W., 2014. Protein aggregation and particle formation in prefilled glass syringes. J. Pharm. Sci. 103 (6), 1601–1612. https://doi.org/10.1002/jps.23973.
Ghazvini, S., Kalonia, C., Volkin, D.B., Dhar, P., 2016. Evaluating the role of the air-solution interface on the mechanism of subvisible particle formation caused by mechanical agitation for an IgG1 mAb. J. Pharm. Sci. 105 (5), 1643–1656. https://doi.org/10.1016/j.xphs.2016.02.027.
Gil, D., Schrum, A.G., 2013. Strategies to stabilize compact folding and minimize aggregation of antibody-based fragments. Adv. Biosci. Biotechnol. 04 (04), 73–84. https://doi.org/10.4236/abb.2013.44a011.
Goldberg, D.S., Bishop, S.M., Shah, A.U., Sathish, H.A., 2011. Formulation development of therapeutic monoclonal antibodies using high-throughput fluorescence and static light scattering techniques: role of conformational and colloidal stability. J. Pharm. Sci. 100 (4), 1306–1315. https://doi.org/10.1002/jps.22371.
Güngören, M.H., Romeijn, S., Dijkstra, J.A., Crul, M., 2024. Investigating the impact of drone transport on the stability of monoclonal antibodies for inter-hospital transportation. J. Pharm. Sci. 113 (7), 1816–1822. https://doi.org/10.1016/j.xphs.2024.04.002.
Guyader, G.L., Vieillard, V., Mouraud, S., Do, B., Marabelle, A., Paul, M., 2020. Stability of nivolumab in its original vials after opening and handing in normal saline bag for intravenous infusion. Eur. J. Cancer 135, 192–202. https://doi.org/10.1016/j.ejca.2020.04.042.
Hong, P., Koza, S., Bouvier, E.S.P., 2012. Size-exclusion chromatography for the analysis of protein biotherapeutics and their aggregates. J. Liq. Chromatogr. Relat. Technol. 35 (20), 2923–2950. https://doi.org/10.1080/10826076.2012.743724.
ICH, 1999. ICH Topic Q 6 B Specifications: Test Procedures and Acceptance Criteria for Biotechnological/Biological Products Step 5. Note for guidance on specifications: test procedures and acceptance criteria for biotechnological/biological products. https://www.ema.europa.eu/en/documents/scientific-guideline/ich-q-6-b-test-procedures-and-acceptance-criteria-biotechnologicalbiological-products-step-5_en.pdf.
Johnson, A.M., Cunningham, C.J., Arnold, E., Rosamond, W.D., Zègre-Hemsey, J.K., 2021. Impact of using drones in emergency medicine: what does the future hold? Open Access Emerg. Med. 13 (13), 487–498. https://doi.org/10.2147/oaem.s247020.
Kizuki, S., Wang, Z., Torisu, T., Yamauchi, S., Uchiyama, S., 2022. Relationship between aggregation of therapeutic proteins and agitation parameters: Acceleration and frequency. J. Pharm. Sci. https://doi.org/10.1016/j.xphs.2022.09.022.
Koepf, E., Eisele, S., Schroeder, R., Brezesinski, G., Friess, W., 2018. Notorious but not understood: how liquid-air interfacial stress triggers protein aggregation. Int. J. Pharm. 537 (1–2), 202–212. https://doi.org/10.1016/j.ijpharm.2017.12.043.
Le Basle, Y., Chennell, P., Tokhadze, N., Astier, A., Sautou, V., 2020. Physicochemical stability of monoclonal antibodies: a review. J. Pharm. Sci. 109 (1), 169–190. https://doi.org/10.1016/j.xphs.2019.08.009.
Linkuvienė, V., Ross, E.L., Crawford, L.B., Weiser, S., Man, D., Kay, S.C., Kolhe, P., Carpenter, J.F., 2022. Effects of transportation of IV bags containing protein formulations via hospital pneumatic tube system: particle characterization by multiple methods. J. Pharm. Sci. 111 (4), 1024–1039. https://doi.org/10.1016/j.xphs.2022.01.016.
Luo, Y., Raso, S.W., Gallant, J., Steinmeyer, C., Mabuchi, Y., Lu, Z., Entrican, C., Rouse, J. C., 2017. Evidence for intermolecular domain exchange in the Fab domains of dimer and oligomers of an IgG1 monoclonal antibody. MAbs 9 (6), 916–926. https://doi.org/10.1080/19420862.2017.1331803.
Malvern, 2013. Zetasizer Nano User Manual (Man0485-1.1). https://www.chem.uci.edu/~dmitryf/manuals/Malvern%20Zetasizer%20ZS%20DLS%20user%20manual.pdf.
MHRA, 2017. Rules and Guidance for Pharmaceutical Distributors 2017 (the Green Guide). Pharmaceutical Press.
NHS, 2023. Assurance of aseptic preparation of medicines. Www.england.nhs.uk. https://www.england.nhs.uk/long-read/assurance-of-aseptic-preparation-of-medicines/.
NHS England, 2018. Dose Banded Chemotherapy Standardised Product Specification – Nivolumab 50ml and 100ml infusion bags. https://www.england.nhs.uk/wp-content/uploads/2018/03/nivolumab-infusion-banded-chemotherapy-standardised-product-spec.pdf.
Nobbmann, U., Connah, M., Fish, B., Varley, P., Gee, C., Mulot, S., Chen, J., Zhou, L., Lu, Y., Sheng, F., Yi, J., Harding, S.E., 2007. Dynamic light scattering as a relative tool for assessing the molecular integrity and stability of monoclonal antibodies. Biotechnol. Genet. Eng. Rev. 24 (1), 117–128. https://doi.org/10.1080/02648725.2007.10648095.
Oakey, A., Grote, M., Smith, A., Cherrett, T., Pilko, A., Dickinson, J., AitBihiOuali, L., 2022. Integrating drones into NHS patient diagnostic logistics systems: Flight or fantasy? PLOS ONE 17 (12), e0264669. https://doi.org/10.1371/journal.pone.0264669.
Oakey, A., Waters, T., Zhu, W., Royall, P.G., Cherrett, T., Courtney, P., Majoe, D., Jelev, N., 2021. Quantifying the effects of vibration on medicines in transit caused by fixed-wing and multi-copter drones. Drones 5 (1), 22. https://doi.org/10.3390/drones5010022.
Rabe, M., Verdes, D., Seeger, S., 2011. Understanding protein adsorption phenomena at solid surfaces. Adv. Colloid Interface Sci. 162 (1–2), 87–106. https://doi.org/10.1016/j.cis.2010.12.007.
Ripple, D.C., Dimitrova, M.N., 2012. Protein particles: what we know and what we do not know. J. Pharm. Sci. 101 (10), 3568–3579. https://doi.org/10.1002/jps.23242.
Roberts, C.J., 2014. Therapeutic protein aggregation: mechanisms, design, and control. Trends Biotechnol. 32 (7), 372–380. https://doi.org/10.1016/j.tibtech.2014.05.005.
Santillo, M., Davies, L., Autsin, P., Campbell, C., Castano, M., Marks, C., 2021. Standard Protocol for Deriving and Assessment of Stability – Part 2: Aseptic Preparations (Biopharmaceuticals). NHS. https://www.sps.nhs.uk/wp-content/uploads/2017/03/Stability-Part-2-Biopharmaceuticals-v5.pdf.
Scherer, T.M., Leung, S., Owyang, L., Shire, S.J., 2012. Issues and challenges of subvisible and submicron particulate analysis in protein solutions. AAPS J. 14 (2), 236–243. https://doi.org/10.1208/s12248-012-9335-8.
Singh, S.K., Afonina, N., Awwad, M., Bechtold-Peters, K., Blue, J.T., Chou, D., Cromwell, M., Krause, H.-J., Mahler, H.-C., Meyer, B.K., Narhi, L., Nesta, D.P., Spitznagel, T., 2010. An industry perspective on the monitoring of subvisible particles as a quality attribute for protein therapeutics. J. Pharm. Sci. 99 (8), 3302–3321. https://doi.org/10.1002/jps.22097.
Some, D., Amartely, H., Tsadok, A., Lebendiker, M., 2019. Characterization of proteins by size-exclusion chromatography coupled to multi-angle light scattering (SEC-MALS). J. Visual. Exp. 148. https://doi.org/10.3791/59615.
Sreedhara, A., Glover, Z.K., Piros, N., Xiao, N., Patel, A., Kabakoff, B., 2012. Stability of IgG1 monoclonal antibodies in intravenous infusion bags under clinical in-use conditions. J. Pharm. Sci. 101 (1), 21–30. https://doi.org/10.1002/jps.22739.
Stetefeld, J., McKenna, S.A., Patel, T.R., 2016. Dynamic light scattering: a practical guide and applications in biomedical sciences. Biophys. Rev. 8 (4), 409–427. https://doi.org/10.1007/s12551-016-0218-6.
Stierlin, N., Risch, M., Risch, L., 2024. Current advancements in drone technology for medical sample transportation. Logistics 8 (4), 104. https://doi.org/10.3390/logistics8040104.
Surman, K., Lockey, D., 2024. Unmanned aerial vehicles and pre-hospital emergency medicine. Scand. J. Trauma, Resus. Emerg. Med. 32 (1). https://doi.org/10.1186/s13049-024-01180-7.
Telikepalli, S.N., Kumru, O.S., Kalonia, C., Esfandiary, R., Joshi, S.B., Middaugh, C.R., Volkin, D.B., 2014. Structural characterization of IgG1 mAb aggregates and particles generated under various stress conditions. J. Pharm. Sci. 103 (3), 796–809. https://doi.org/10.1002/jps.23839.
THE MODEL SHOP. (n.d.). 110 LBF ELECTRODYNAMIC EXCITER. THE MODEL SHOP. https://www.modalshop.com/docs/themodalshoplibraries/datasheets/2110e-110-lbf-electrodynamic-exciter-datasheet-ds-0078.pdf?sfvrsn=4131d00c_7.
Theobald, K., Zhu, W., Waters, T., Cherrett, T., Oakey, A., Royall, P.G., 2023. Stability of medicines transported by cargo drones: investigating the effects of vibration from multi-stage flight. Drones 7 (11), 658. https://doi.org/10.3390/drones7110658.
Torrente-López, A., Hermosilla, J., Salmerón-García, A., Cabeza, J., Navas, N., 2022. Comprehensive analysis of nivolumab, a therapeutic anti-Pd-1 monoclonal antibody: impact of handling and stress. Pharmaceutics 14 (4), 692. https://doi.org/10.3390/pharmaceutics14040692.
US Pharmacopoeia, 2016. <788> PARTICULATE MATTER IN INJECTIONS. https://www.usp.org/sites/default/files/usp/document/harmonization/gen-method/q09_pf_ira_33_2_2007.pdf.
Wiltshire, M., Boxshall, J., Milne, J., Oleniacz, K., Theobald, K., Phillips, B., 2024. The effects of drone transportation on blood component quality: a prospective randomised controlled laboratory study. Br. J. Haematol., Published Online. https://doi.org/10.1111/bjh.19666.
Wozniewski, M., Besheer, A., Huwyler, J., Mahler, H.-C., Levet, V., Sediq, A.S., 2024. A survey on handling and administration of therapeutic protein products in German and Swiss hospitals. J. Pharm. Sci. 113 (3), 735–743. https://doi.org/10.1016/j.xphs.2023.09.010.
Wu, S., Tang, Y., Lin, M., Sneddon, A., 2020. Headspace isotope & compositional analysis for unconventional resources: gas in place, permeability and porosity prediction and completions planning. Geosciences 10 (9), 370. https://doi.org/10.3390/geosciences10090370.
Zhu, W., Oakey, A., Royall, P.G., Waters, T.P., Cherrett, T., Theobald, K., Bester, A.-M., Lucas, R., 2023. Investigating the influence of drone flight on the stability of cancer medicines. PLOS ONE 18 (1), e0278873. https://doi.org/10.1371/journal.pone.0278873.